INFORMATION TO USERS

This manuscript has been reproduced from the microfilm master. UMI films the text directly from the original or copy submitted. Thus, some thesis and dissertation copies are in typewriter face, while others may be from any type of computer printer.

The quality of this reproduction is dependent upon the quality of the copy submitted. Broken or indistinct print, colored or poor quality illustrations and photographs, print bleedthrough, substandard margins, and improper alignment can adversely affect reproduction.

In the unlikely event that the author did not send UMI a complete manuscript and there are missing pages, these will be noted. Also, if unauthorized copyright material had to be removed, a note will indicate the deletion.

Oversize materials (e.g., maps, drawings, charts) are reproduced by sectioning the original, beginning at the upper left-hand corner and continuing from left to right in equal sections with small overlaps.

Photographs included in the original manuscript have been reproduced xerographically in this copy. Higher quality 6" x 9" black and white photographic prints are available for any photographs or illustrations appearing in this copy for an additional charge. Contact UMI directly to order.

Bell & Howell Information and Learning
300 North Zeeb Road, Ann Arbor, MI 48106-1346 USA
800-521-0600

Discrete Cascade Universal Multifractal Simulation and Analysis

R.W. Nowak, Physics Dept.
McGill University, Montréal
June 1999

A thesis submitted to the Faculty of Graduate Studies and Research in partial fulfillment of the requirements of the degree of Master of Science.

abstract

Historically discrete multiplicative cascade models have been developed to mimic some of the characteristics of fully-developed turbulence. Some of these models have been found to be of much more general relevancy and have been used to simulate and analyse many different kinds of simple geophysical and other scaling fields. The desire to describe more complex processes has led to the invention of multivariate multiplicative cascade models. Of these the simple "complex cascade model" is considered in detail in this thesis. The background theory of Lévy random variables and discrete scalar cascades is covered and a description of the various existing analysis techniques is provided. Two analysis techniques are described and tested on complex cascade simulations. The new "adjacent data points" (ADP) method is found to be superior to the traditional analysis technique. A discussion of the difficulties which may be encountered when analysing recorded complex data is included.

résumé

Historiquement, les modèles de cascade multiplicative ont été développés pour simuler certaines des caractéristiques de la turbulence pleinement développée. Quelques-uns de ces modèles se sont avérés d'une pertinence dépassant les limites de la turbulence et ont ainsi été utilisés pour simuler et analyser plusieurs champs géophysiques simples ainsi que d'autres champs possédant une invariance d'échelle. La volonté de décrire des processus plus complexes a mené à l'invention des modèles de cascade multiplicative à plusieurs variables. Parmi ceux-ci, le modèle simple de cascade complexe est étudié en détail dans ce mémoire. Les fondements de la théorie des variables aléatoires de Lévy ainsi qu'une description des différentes techniques d'analyse sont présentés. Deux techniques d'analyse sont décrites et vérifiées par des simulations de cascades complexes. La supériorité de la nouvelle méthode des points adjacents par rapport à la méthode d'analyse standard a été démontrée. Une discussion sur les difficultés qui peuvent se présenter lors de l'analyse de données complexes est incluse.

Foreword

He is God, no God is there but Him,
the All-Merciful, the Compassionate.

This thesis marks the end of four years hard work on various projects which taught me a great deal. The fruit of my work on the basic theory of the discrete multifractal simulation can be found here in these pages. Not all of it made it though, the requirement that a masters thesis be a light-weight self-contained unit of less than 101 pages has meant a difficult censorship of those parts of the theory which strayed even slightly from the well-beaten path. I hope that you will find the learning and results presented here to be informative and useful, and above all clearly written.

It is customary to thank various individuals who have made a significant contribution to the life and work of the author. So it would be negligence on my part not to say how grateful I am to the effort put in by Feller, Zolotarev and Samorodnitsky & Taqqu in writing their classic books on statistics. It would also be wrong not to say how much I have been helped by my colleagues and friends during the time I spent in Montréal. I will not try to name all of them but, of the former, Nicolas Desaulniers-Soucy, Philippe Sagar, Badrinath Nagarajan & Ramón de Elía, and of the latter, Shahab Akhound-Zadeh-Miandoab and Jeff Zaat must be mentioned for their sparkling qualities. Also Martin Grant has been extremely generous with his time in agreeing to read through my thesis on several occasions to give his useful comments.

Finally, the dedication of my supervisor to his work must be acknowledged here; along with Daniel Schertzer, Shaun Lovejoy has developed the manifold theories on which this thesis is based and he must be thanked for this. The only original contributions of my own to the mathematics have been the ADP analysis method of chapter III and the explanations for the limitations of the complex analysis in § III.6.

R.W. Nowak
Montréal, 14 June 1999

Contents

Glossary (of commonly used terms)

eqn.	equation
fig.	figure
m.f.	multifractal
p.d.f.	probability density function
r.v.	random variable
ADP	adjacent data point(s)
DCUM	discrete cascade universal m.f.
S&L	Schertzer & Lovejoy (1995)
S&T	Samorodnitsky & Taqqu (1994)
$\langle\ \rangle$	average, defined for a r.v. x with p.d.f $p(x)$ as $\langle x \rangle = \int_{-\infty}^{\infty} x\, p(x)\, dx$
$c(\gamma)$	"codimension function," defined in equation (I.10)
d	dimension of (embedding) space
q	exponent, usually real and positive; "order of moment"
C_1	"codimension of the mean," § II.2.4
D_B	"box-counting (fractal) dimension," defined in equation (I.8)
K(q)	"(Laplace) second characteristic function," defined in § II.2.3
K(q)	"moment scaling function," defined in equation (II.8)
L	"outer scale," the size of box in which the whole process will fit
$Z(q)$	"(Fourier) characteristic function," § II.2.3
α	a parameter in the α-model of § I.4.2
α	"Lévy index" of a Lévy r.v., § II.2.3
β	a parameter in the β-model of § I.4.1
β	"skewness parameter" of a Lévy r.v., § II.2.3
β	slope of power spectrum, defined in equation (II.9)
ε_λ	(the value of a) field (at a point in space and time) at resolution λ
γ	"order of singularity," § II.2.1
λ	"resolution" or "scale" corresponding to a physical size of L/λ
μ	"shift parameter" of a Lévy r.v., § II.2.3

I Introduction

I.1 The Limitation of Human Prescience

The origins of science itself can be found at the time c. 3500-2500 BC, known by historians as the period of the hieratic city state[1]. The people of that time conceived of the city as an imitation on earth of the cosmic order which they observed around them. Administered by the priests and other classes the universe, society and the individual were made to be in perfect harmony. One of the chief rôles of the priests, then, was to make highly accurate observations of nature so that they could ensure that man continued to be in consonance with the cosmos. Well-known examples of the skill with which such observations were made are the pyramids and Stonehenge. And this was the birth not only of science but also writing, the wheel, mathematics, the calendar, astronomy, number systems (decimal and sexigesimal), kingship, the class system, priestcraft, taxation and bookkeeping. The important idea underlying all this is that nature was believed to be perfect and divine and science was in accord with religion. Indeed the purpose of science itself was very much diagnostic, if not predictive.

This view persisted for approximately 5000 years until finally a rift began to appear between the two. The European Christians having inflated Revelation beyond reason were delivered their first blow by William of Ockham (c. 1300-1349) with his so-called Ockham's razor. Then, starting with Kopernik[2] (a.k.a. Copernicus) in 1507 and culminating with Galileo, the priests (of the Roman Catholic Church, in 1630) marked the departure of the two by condemning as heresy Galileo's scientific discovery that the earth moves round the sun. Thus science was cut from the root by those who were there to tend it. And alone but confident, like a rebellious adolescent, it was seemingly capable of anything. So as the importance of the priests diminished the achievements of man's use of reason seems to have grown exponentially.

Among the great scientific discoveries of those times was Newtonian physics which was an important part of the eighteenth-century Enlightenment and Industrial Revolution. In fact (classical) mechanics became the first physical theory to be studied systematically. It

seemed that there could be no limit to the technological and scientific achievements possible[3]. Science progressed with mechanics, fluids and then electricity and on to particles. Finally, after about 250 years of this new found freedom a few truly astonishing scientific discoveries made it clear that there were severe and restrictive limitations on what man could hope to achieve. The theory of relativity (special theory in Einstein (1905)), the uncertainty of quantum mechanics (starting with Planck (1900)) and Gödel's incompleteness theorem (Gödel 1931) are some of the outstanding examples of scientific and mathematical discoveries which irrevocably proved the by then five-and-a-half-millennium-old idea of absolute knowledge to be inadequate. This was perhaps the most fundamental change in our *weltanschauung*, a change which we are unlikely to see repeated in our own lifetimes. From the broken hubris of our past it was up to the open-minded scientists to construct a new way of looking at things.

Fig. I.1: Mikolaj Kopernik (picture from O'Connor & Robertson 1999)

But the cracks had already started to appear during the last century. One such example was the discovery, over a hundred years ago by Poincaré (1892), that mechanical systems which followed Hamilton's equations could display chaotic motion. It was not until much more recently that in our particular field of interest Lorenz (1963) discovered deterministic chaotic behaviour in a very simple mathematical model of convection in a fluid layer heated from below. He found that his set of three coupled total differential equations

permitted solutions in a particular parameter range for which the model had exponential sensitivity to initial conditions. What made the discovery so important is that the observed chaotic behaviour in time is not due to noise, or an infinite number of degrees of freedom, or quantum mechanics. It was thus shown that our ability to determine future events in a deterministic world has its limitations.

I.2 An Investigation of Vortices and Turbulence

The detached and secular observation of nature started with the Greeks. In their writings can be found descriptions of such natural phenomena as whirlwinds and dust devils. About 1500 years later Leonardo da Vinci (1452-1519) reached a sort of culmination in the artistic description of such natural events. His drawings contain many examples of turbulent and vortical flow in channels and around obstacles. The smooth flow of a fluid around a cylinder, for example, is called laminar flow. As the flow speed is increased vortices begin to appear in the cylinder's wake. At higher flow speeds the vortices form and detach repeatedly, flowing with the fluid behind the cylinder in the so-called Kármán vortex street (see fig. I.2, top). Finally at even higher flow speeds the fluid motion behind the cylinder becomes entirely chaotic: this is called (fully developed) turbulent flow and the mechanism which has just been described is called transition through spectral development. This progression may be seen in figure I.2 below (the parameter R will be defined in § I.3.1) from top to bottom.

A different kind of transition from laminar to turbulent flow was first described by Reynolds (1883). In his experiments water was introduced into a pipe at a constant flow rate within which there was a thin stream of highly coloured water (tracer) to make the flow pattern discernible. At low speeds the flow remained laminar throughout the length of the pipe as could be seen by observing a straight line marked by the tracer. When the flow rate was increased beyond a critical value he found that at a certain distance from the entrance to the pipe the thin line of tracer fluid suddenly broadened out to fill the entire cross-section of the pipe (see figure I.3). The mixing of the tracer indicated a sudden transition to strongly turbulent flow. This abrupt transition is caused by small instabilities in the flow which get

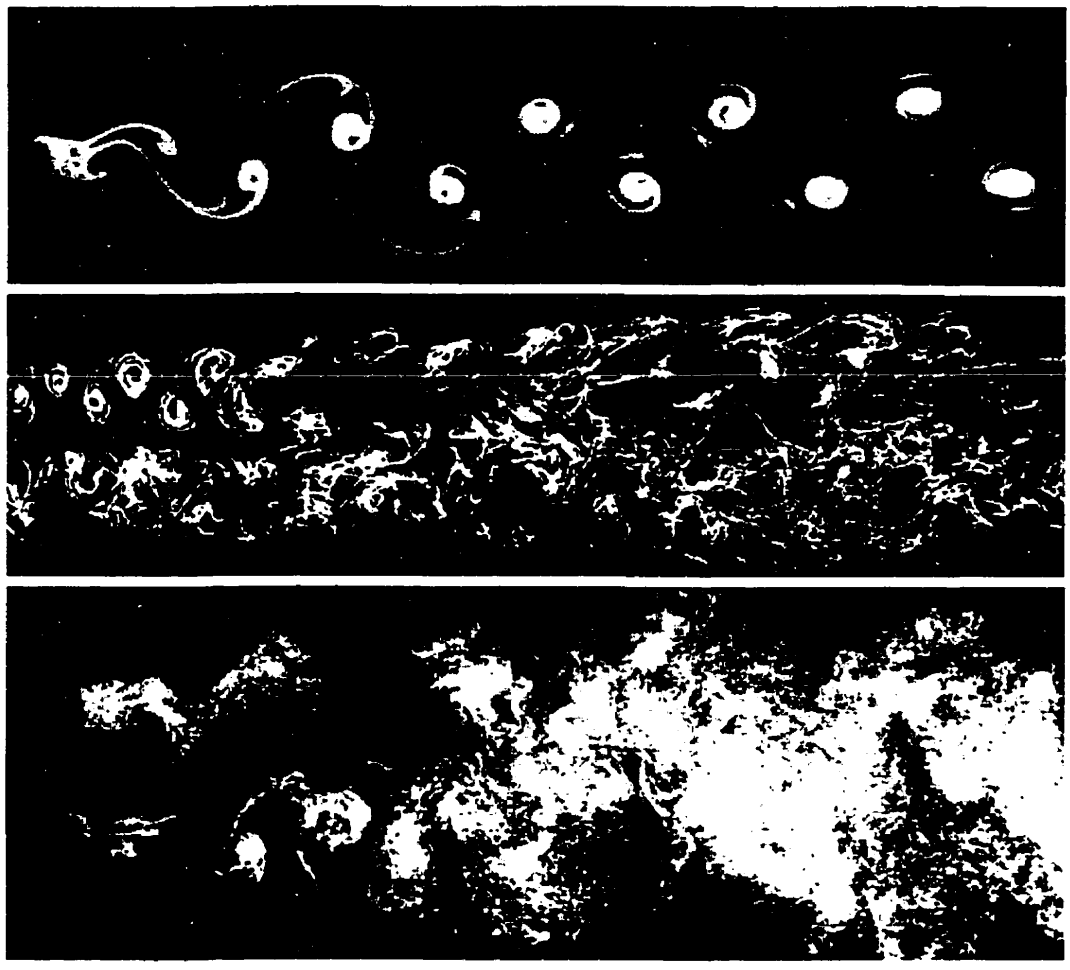

Fig. I.2: Some steps in the progression from laminar flow to fully developed turbulence; the pictures show (top) the wake behind a single cylinder for R=105 and behind two identical cylinders for R=240 & 1800 (middle and bottom, respectively). Pictures from (top) Van Dyke (1982) and (bottom & middle) Frisch (1995).

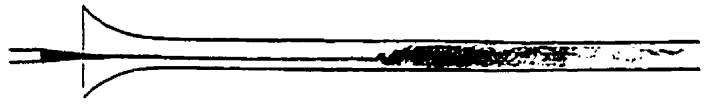

Fig I.3: Reynolds' pipe flow experiment showing the sudden onset of turbulence after a period of laminar flow as seen in the tracer mixing with the water, flowing from left to right (fig. from Reynolds 1882).

amplified, and is exactly like the sensitive dependence on initial conditions found by Lorenz (§ I.1). In an analogous way the instabilities in the (much more complex) atmosphere become amplified and lead to turbulence and the manifold natural phenomena which are seen as a result[4].

Leonardo da Vinci was the first to describe turbulent fluid motion[5]. Today it might be said that fully developed turbulence has the following basic properties (as adapted from Warn (1995)): a complex space-time structure involving a broad range of scales; irreproducibility—repeated experiments yield different outcomes, hence a lack of predictability; high levels of vorticity; strong dissipation and rapid decay after energy sources are removed; enhanced transport properties. It could also be said that turbulence is deterministic, because the physical laws governing its motion are known exactly. But with the sensitive dependence on initial conditions and the very large number of degrees of freedom it is difficult in practice to make this work in general[6]. The limited success of numerical weather prediction models is in large part due to this.

Indeed, of the five review articles consulted in the writing of this chapter the biggest commonality they share is their agreement that the theoretical understanding and quantification of turbulence is a problem which is still far from being solved (eg., Bhattacharjee's (1998) review focuses on this aspect in particular). Thus with the chaotic uncertainties of turbulence it seems natural to wonder whether a probabilistic description is justified; the answer is certainly yes (eg., Frisch (1995) p. 57). The paper "Statistical Theory of Turbulence" (58 pages in four parts) by Taylor (1935) was pioneering work in this regard. He suggested for the first time that the oscillations of the atmospheric velocity field be measured statistically and used to compute the energy spectrum. This was soon followed by much research by others.

I.3 Reynolds, the Navier-Stokes Equation and Kolmogorov

I.3.1 The Navier-Stokes equation

The equations of motion applied to an inviscid fluid were derived in the period 1752-1759 by Euler, and are now known as Euler's equation. About seventy years later an additional viscous term in this equation was derived for viscous fluids. For a Newtonian fluid of constant viscosity, and with the simplification of assuming that the fluid is also incompressible, the result is called the Navier-Stokes equation and has been known since Navier (1823). It is

$$\frac{d\underline{v}}{dt} = -\frac{1}{\rho}\underline{\nabla} p + \upsilon \nabla^2 \underline{v} + \underline{f} \qquad \text{(I.1)}$$

where $\underline{v}$, p, ρ and υ are the velocity, pressure, (constant) density and (constant) kinematic viscosity of the fluid respectively. $\underline{f}$ represents body forces such as stirring or gravity, though these are usually neglected as shall be done below.

Some very important observations must be made about this equation (I.1) of motion as it forms the basis of later work dealing with turbulent fluid flow.

Firstly the Navier-Stokes equation (I.1) can be non-dimensionalised to reveal a dependence on just one parameter. By choosing a characteristic length and velocity scale (eg., in Reynolds' pipe flow experiment these were the size of the pipe and the flow speed) the dimensionless position and velocity vectors can be written as

$$\underline{r'} = \frac{\underline{r}}{L} \text{ and } \underline{v'} = \frac{\underline{v}}{U}.$$

The remaining variables may be dealt with similarly by introducing arbitrary scales (constants) which may be set to any value, ultimately thereby allowing a reduction in the number of parameters. These are

$$t' = \frac{t}{T} \text{ and } p' = \frac{p}{P}.$$

Introducing the dimensionless variables into (I.1) gives

$$\frac{L}{VT}\frac{d\underline{v'}}{dt'} = -\frac{P}{V^2\rho}\underline{\nabla'} p + \frac{\nu}{VL}\nabla'^2 \underline{v'}$$

which can be simplified by choosing $T = L/U$ and $P = \rho V^2$ to give the dimensionless Reynolds equation

$$\frac{d\underline{v'}}{dt'} = -\underline{\nabla'} p' + \frac{1}{R}\nabla'^2 \underline{v'} \qquad \text{(I.2)}$$

where the single (dimensionless) parameter R is given by

$$R = \frac{UL}{\upsilon}.$$

In this form equation (I.2) has only one parameter, R, called the Reynolds number which depends only on the characteristic scale and velocity of the flow and inversely on the (kinematic) viscosity of the fluid. As a consequence it was noted by Reynolds (1883) that two different configurations of the system may be dynamically similar if their Reynolds numbers are equal. And, in particular, he noticed (§ I.2) that the determining factor as to whether turbulence occurs or not is the value of R; flows with R above a critical value will be turbulent. This critical value for pipe flow is about 2300. This should be compared with the Reynolds number of the atmosphere (for which the large scale phenomena have $U \approx 10$ ms^{-1}, $L \approx 1000$ km and $\upsilon \approx 10^{-5}$ m^{2}s^{-1}) which is somewhere of the order 10^{12} ie., very much larger. In fact such a large value of Reynolds number is as yet impossible to achieve either in experiment or numerical simulation.

Secondly the Navier-Stokes equation has several inherent symmetries which, ignoring boundaries, are invariance under space and time translation, rotation, parity (space and velocity reversal) and scaling transformations. The geometric symmetries are easily witnessed in laminar flow but as the onset of fully developed turbulence is approached, and the smoothness of the flow is disrupted, these symmetries begin to break (eg. the up-down symmetry of the Kármán vortex street in fig. I.2 lacks a left-right symmetry). Finally when the turbulence is fully established it is observed to be homogeneous and isotropic (already implied in Kelvin (1887) but not tested experimentally until much later eg., isotropy by Townend (1934)); the geometric invariances are once more established, at small scales and away from boundaries, in a statistical sense. Of the scaling property of the Navier-Stokes equation consider the isotropic transformations

$$\underline{x} \to \lambda \underline{x} \text{ and } \underline{v} \to \lambda^h \underline{v}, \tag{I.3}$$

where h is an arbitrary scaling exponent. These already imply that $t \to \lambda^{1-h} t$. Substituting these into equation (I.1) reveals that the scaling of the remaining variables must be $\upsilon \to \lambda^{1+h} \upsilon$ and $\underline{f} \to \lambda^{2h-1} \underline{f}$.

I.3.2 The seeds of Kolmogorov's 1941 papers

Assuming homogeneity and isotropy, for sufficiently large Reynolds number and at small scales away from boundaries and singularities, Kolmogorov[7] (1941a) made his two hypotheses of similarity. His second hypothesis of similarity essentially states that the statistical properties of (fully-developed) turbulence at scales larger than the dissipation scale, the finest scale at which most energy is lost to viscosity, are dependent only on the mean dissipation rate $\bar{\varepsilon}$ (and not on υ). So consider the statistics of the (longitudinal) velocity differences $\Delta v(l) = v(x+l) - v(x)$ and the corresponding velocity structure function

$$B_q(l) = \left\langle (\Delta v(l))^q \right\rangle \tag{I.4}$$

(where $\langle\ \rangle$ indicates taking the mean of the quantity inside the brackets). Since $\bar{\varepsilon}$ has dimensions of $[L]^2[T]^{-3}$ further dimensional analysis shows that Kolmogorov's second hypothesis implies

$$B_q(l) = C_B \bar{\varepsilon}^{q/3} l^{q/3} \tag{I.5}$$

where C_B is a universal dimensionless constant[8]. This result was derived for q=2 (the second order velocity structure function, for which the exponent on l is two thirds) in Kolmogorov (1941a) and is known as the "two-thirds law." Considering once again the scaling transformations (I.3) it can be seen that the LHS of (I.5) changes by a factor of λ^{qh} when transformed whereas the RHS changes by a factor $\lambda^{q/3}$; therefore $h = 1/3$. Equation (I.4) may be rewritten in a more general form for the magnitude of the velocity differences

$$S_q(l) = \left\langle |\Delta v(l)|^q \right\rangle \propto l^{\zeta(q)} \tag{I.6}$$

where Kolmogorov's second hypothesis of similarity implies that

$$\zeta(q) = \frac{q}{3}. \tag{I.7}$$

The prediction that the velocity structure function of order q will exhibit scaling in the inertial range with scaling exponent $\zeta(q) = \frac{1}{3}q$ (a linear behaviour in q) is amenable to

Fig. I.4: Andrei N. Kolmogorov (picture from Kendall 1990)

experimental testing of different order moments. But it should be noted that in his 1941 papers Kolmogorov only gave explicit predictions for the second and third order moments, and that measurements of higher order moments is difficult. This may be why no tests were performed with $q \geq 4$ until Van Atta & Chen (1970). Since then improved investigations have been made eg., Anselmet et al. (1984), Arneodo et al. (1996), Benzi et al. (1993) and Schertzer et al. (1995)[9]. Notably it has been found that the structure function exponent deviates significantly from this scaling relationship (I.7) at higher order moments: an effect known as "anomalous scaling." This will be the subject of more discussion in § I.5.

Another implication of Kolmogorov's second hypothesis may be seen by considering that energy has dimensions of $[L^3][T^{-2}]$. Thus the energy spectrum will be given by $E(k) = C_E \bar{\varepsilon}^{2/3} k^{-5/3}$. This result was first seen explicitly in an independent derivation by Oboukhov (1941) and consequently is known as the "Kolmogorov-Oboukhov five-thirds law". The landmark experiment in verifying the five-thirds power law behaviour was due to Grant et al. (1962) who analysed tidal channel data to convincingly show the predicted power law over a scale ratio of approximately 10^3. This has been, and continues to be, the subject of much investigation (for good reviews see Lilly (1983) and Schertzer and Lovejoy (1983) and controversy over such points as the putative meso-scale gap (since Van der

Hoven 1957) which is associated with the separation of the regimes of two and three-dimensional turbulence in the atmosphere. Despite the controversies it would seem that with ever increasing computing power and improvements in measuring devices the range and quality of unbroken scaling seen in turbulent fluids only increases. (Indeed, as an aside, the scaling behaviour observed in energy spectra has become rather ubiquitous in measurements of natural phenomena of all kinds.) However the power spectrum is itself a second-order moment (the Fourier transform of the autocovariance) and does not paint the entire picture of the nature of turbulence.

One important aspect of the character of fully developed turbulence which had been almost totally ignored is the intermittency of turbulent fields. In particular the rate of energy dissipation is not constant throughout space and time. Twenty one years after his 1941 turbulence papers Kolmogorov (1962) made a third hypothesis that the rate of dissipation is lognormally distributed in space and time. This followed Oboukhov (1962) who had assumed the same (but only) for pragmatic reasons, and a criticism by Landau (of Kolmogorov's 1941 work) that theoretically there is an increase without limit of the dissipation as the ratio of scales increases. Thus the notion of intermittency, or "spatial inhomogeneity" as Batchelor & Tonwnsend (1949) called it, was formally taken up in the mathematics and the question of what statistics may best describe these fluctuations was raised[10]. Indeed the first to propose a type of intermittency model already markedly different to the ideas in Kolmogorov (1962) were Novikov & Stewart (1964).

I.4 Scaling, Cascades and Phenomenological Models

I.4.1 Cascades and intermittency; early models

Kolmogorov (1962) states that "the hypotheses concerning the local structure of turbulence at high Reynolds number, developed in the years 1939-41 by myself and Oboukhov were based physically on Richardson's idea of the existence in the turbulent flow of vortices on all possible scales... and of a certain uniform mechanism of energy transfer from the coarser-scaled vortices to the finer." It would now do well to recall that Richardson[11] was himself the pioneer of numerical weather prediction and in Richardson (1922) there appeared the now famous poem

Fig. I.5: Lewis F. Richardson (picture from O'Connor & Robertson 1999)

Big whorls have little whorls,
That feed on their velocity;
And little whorls have smaller whorls,
and so on to viscosity.

This poem, it turns out, makes a good model for fully developed turbulence when taken quite literally. The energy of the largest eddies, at the so-called outer scale or sometimes injection scale, is successively passed down to smaller eddies of a similar size (localness of interactions) until finally, having traversed the entire range of scales, the dissipation scale is approached where most of the energy is lost through dissipation. The important features of this model are that i) it is a self-similar cascade process, which means that the operation taking place at the large scales is the same as the one taking place at the small scales, and ii) the fundamental quantity of interest, which is itself conserved in the cascade process, is the energy flux ε. (Indeed it is probable that thinking along such lines is what led Kolmogorov (1941a) to make his two hypotheses of similarity.)

It is the energy flux, then, which became the subject of much attention in the form of self-similar cascade models. Of course such models were considered for probabilistic

rather than deterministic purposes. The first explicit self-similar cascade models were by Novikov & Stewart (1964) and Yaglom (1966). Whereas the latter was manifestly interested in the lognormality of the distribution of intermittency, by making use of Kolmogorov's third hypothesis (the "log-normal model"), the former were concerned with the patchiness in a literal sense as their model contained patches which either contained energy or were entirely devoid of it (the "black-and-white model"). As such this was quite an extreme departure from being realistic in the sense of being able to generate fields which had the appearance of an actual turbulent field.

It should be noted that intermittency can occur as the result of simple repeated scaling operations applied to geometrical shapes in two dimensions eg., Von Koch curves (Von Koch 1906), or one dimension as in the Cantor set (Cantor 1883). The latter, long known by mathematicians as a sort of pathological construction thanks to its harsh intermittency, forms what is known as a Cantor dust when carried through to infinitely small scales. Hence, as intermittency is observed in nature, it would seem that there is reason to pursue models of turbulence based on this sort of construction. Mandelbrot's (1967) historic paper introduced the usefulness of the concept of fractals[12], (loosely) complicated geometrical objects of fractional dimension, as pertaining to the question "How long is the coast of Britain?" Although there are various different ways of defining what a fractal is, here it is sufficient to adopt the (still rather woolly) definition that a fractal is a complicated shape (set of geometric objects) whose effective dimension is greater than the topological dimension of the basic material it is constructed from eg., dots, lines etc. Note that this definition is consistent with the idea that a fractal is not space filling ie., that it has a fractional dimension less than that of the embedding space.

As an example of a fractal consider the triadic Cantor set shown in figure I.6 which is shown in various stages of construction (going down the page). It is made from a one-dimensional bar which is repeatedly split into two smaller parts, then two into four etc.: it is self-similar. In the limit of an infinite number of such operations it is a set of points which (individually) have a topological dimension of zero separated by gaps of all (only at discrete intervals) length scales. Notice that this particular set is not space filling: the

intermittency which is seen in the Cantor set is a characteristic of fractals which are not space-filling.

The effective dimension of this construction may be given, for example, by the simple "box-counting method" (eg., Meakin 1998). The box-counting dimension for a fractal lying in d-dimensional space is defined as

$$D_B = \lim_{l \to 0} \frac{\log N(l)}{\log(1/l)} \tag{I.8}$$

where $N(l)$ is the number of non-empty, d-dimensional hypercubes filling the space, each of side l. Though in practice the limit $l \to 0$ is not taken; the ratio (I.8) is evaluated at a number of different scales for which $N(l)$ is very large. For the triadic Cantor bar, at the nth level down, $l = (1/3)^n$ and $N(l) = 2^n$ which gives a box-counting dimension (independent of n) of $D_B = \log 2/\log 3 \approx 0.631$. This exceeds the topological dimension and, by the loose definition adopted above, is the fractal dimension of the triadic Cantor bar.

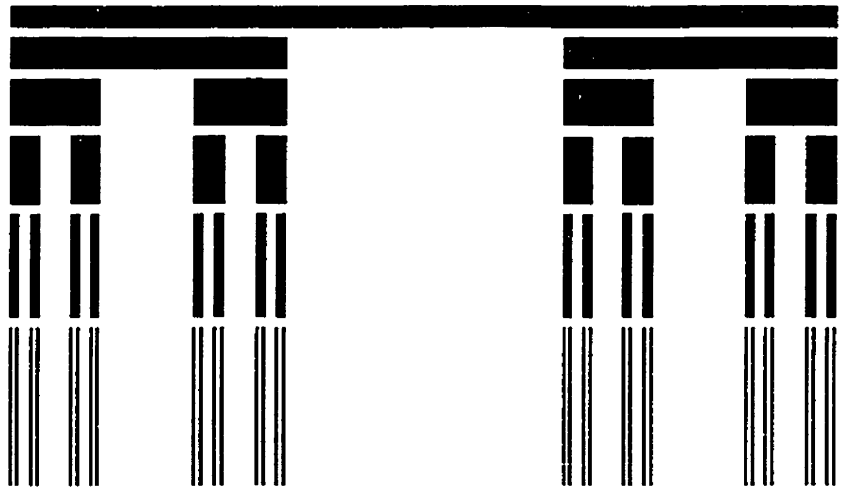

Fig. I.6: Triadic Cantor bar constructed by successively removing the middle third from each black bar (going down the page). Here the height of each bar, representing intensity, is such that the sum total area of the bars across any horizontal level is a constant; the area is conserved. Note that there is also an increase in intensity, accompanied by a decrease in the width of the bars, demonstrating the increasing intermittency of the system going towards smaller scales (fig. from Feder 1988).

Equation (I.8) may be rewritten by defining the quantity $\lambda = 1/l$ (commonly called the "scale" or "resolution") to give $N(1/\lambda) = \lambda^{D_B}$. So the probability that a hypercube of scale λ is not empty is

$$P_\lambda = \frac{N(1/\lambda)}{\lambda^d} = \lambda^{D_B - d}$$

$$P_\lambda = \lambda^{-c} \qquad (I.9)$$

where the quantity $c = d - D_B$ is called the "codimension." If a fractal energy cascade is considered to be a model for turbulence then the effect of a non-zero codimension is to make the scaling exponent for fully-developed turbulence $h = \frac{1}{3}(1 - c)$. (This result may be demonstrated by dimensional analysis considerations eg., Frisch (1995) pp. 138-139, the details of which are not of importance here.) Furthermore this can be shown to imply that the structure function exponent $\zeta(q) = \frac{1}{3}q + c(1 - \frac{1}{3}q)$. This result is an example of anomalous scaling with a linear term in q which results from the non-space-filling properties of a fractal field.

The black-and-white model, rather like a random version of the Cantor bar, produced an intermittency which was not space-filling; it is fractal. Mandelbrot (1974) made a detailed study of the log-normal and black-and-white models arriving at a very general multiplicative cascade scheme which he calls "curdling" and which can be either space-filling or not[13], see figure I.7. (When space filling he called this the "weighted-curdling model," otherwise the "absolute-curdling model.") Related to the black-and-white model Frisch, Sulem & Nelkin (1978) produced a very similar model, intended as a 'toy model,' called the "β-model" (see figure I.8). This model in particular has a codimension of $c = 1 - \log_2 \beta$ which is dependent on the choice of the pameter β ([14]); it too is fractal. But during the period 1982-1983 it became increasingly more obvious that experimental data were not showing the linear dependency (anomalous scaling) of fractal models of turbulence. This prompted the search for other models that could account for this behaviour[15].

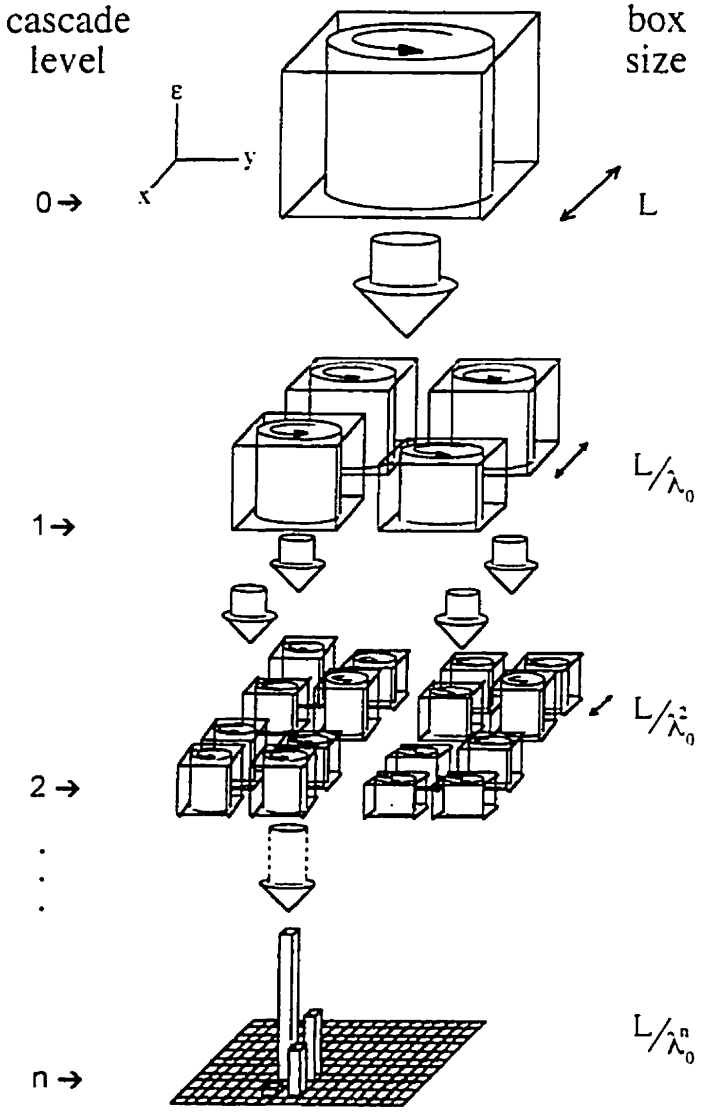

Fig. I.7: Schematic diagram to illustrate the prototypical random multiplicative cascade model in two dimensions. The cascade proceeds from the largest scale L, where the 'eddy' fills the entire space, to the smallest scale L/λ_0^n in n steps; the scale ratio between successive steps is λ_0 . At each step the quantity ε is multiplied by an independent random quantity which may have zero values. This model may be space-filling or not and is the basis for all the discrete cascade models discussed in this section; the only fundamental difference between them being the choice of random multiplicative factor. (Fig. reproduced from Schertzer & Lovejoy (1997) with minor modifications.)

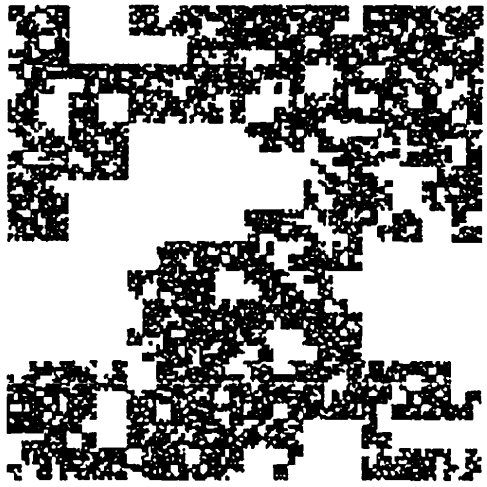

Fig. I.8: A simulation from the β-model in 2-D where the black squares represent "alive" energetic turbulent eddies. At each cascade step every square is divided into four smaller ones and in this case the fraction of squares which are kept alive is $\beta = 2^{-0.2}$=0.871; here there are nine such cascade steps. It can be shown that for the β-model $D_B = 2 + \log_2 \beta$ which gives $D_B = 1.8$. (Fig. from Schertzer & Lovejoy 1996)

I.4.2 Multiscaling and multifractal models

By considering the characterization of strange attractors by their (fractal) dimension, something which up until that point had been limited to only three truly different dimensions[16], Hentschel & Procaccia (1983) showed that strange attractors are in fact characterized by an infinite number of generalized (fractal) dimensions. At about the same time the idea that intermittency in fully developed turbulence may be characterised by many (or a hierarchy of) fractal dimensions can be found in Schertzer & Lovejoy (1984) and Parisi & Frisch (1985). In the latter Parisi & Frisch coined the term « multifractal » (m.f. for short) with its obvious meaning. They state the fact that the Navier-Stokes equation is invariant under scaling transformations for any value of the scaling exponent h; h need not remain fixed. This "multiscaling" implies that the codimension is no longer a constant. What this means in practice for a (1-D) field viewed at a resolution λ can be seen in figure I.9. In this figure two exceedence levels are shown which define the set of boxes where the field $\varepsilon_\lambda(x)$ (note that the field is no longer black or white but can take any real positive value) is greater than a certain threshold. These sets of boxes can have fractal dimensions

different from each other thereby allowing the codimension for a field of this type to be many-valued. Thus equation (I.9) may be generalised to

$$\Pr(\varepsilon_\lambda \geq \lambda^\gamma) = \lambda^{-c(\gamma)} \tag{I.10}$$

(Pr means 'the probability that...') where γ is the "order of singularity" and the codimension is now a function of γ.

This idea expressed by Parisi & Frisch (1985) permits anomalous scaling with non-linear terms in q, but as an idea it was without any suggestion as to how to generate such a field. They express the desirability of finding by experiment the departure of $\zeta(q)$ from linearity and also the importance of showing universality in its form ie., that it should be independent of initial conditions and all other parameters which should be irrelevant in fully developed turbulence. It may be added to these points that there is also the unspoken hope that the function $\zeta(q)$ will itself not depend on an infinite number of parameters to specify it.

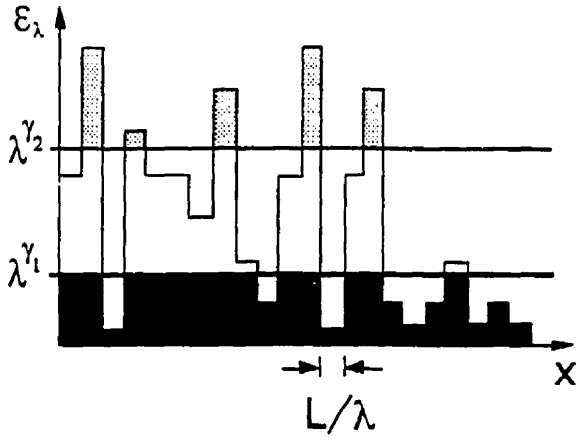

Fig. I.9: A 1-D field seen at a resolution λ with two sets (of line sections) defined by the exceedence levels λ^{γ_1} and λ^{γ_2}; in general the sets may have different fractal dimensions making it a multifractal field. (Fig. reproduced from Schertzer & Lovejoy (1996) with minor modifications.)

Schertzer & Lovejoy (1984) describe the practical, though still pedagogical, "α-model" (actually more clearly elucidated in Schertzer & Lovejoy (1985)) which is a simple enhancement of the β-model. In this weighted curdling, or space-filling, model the

eddies are either increased or decreased (are multiplied by $\lambda^{\gamma} > 1$ or $\lambda^{\gamma} < 1$, respectively, as determined by the choice of the two parameters) at each cascade step by a random choice thus

$$\Pr(\text{increase}, \lambda^{\gamma}) = \beta$$
$$\Pr(\text{decrease}, \lambda^{\gamma}) = 1 - \beta$$

where conservation of the overall mean of the field implies that $\beta\lambda^{\gamma} + (1-\beta)\lambda^{\gamma} = 1$. In this way the field generated after many cascade steps may have many different possible values resulting from the random combination of increases and decreases ie., of "mixed orders of singularity," allowing for the possibility of a hierarchy of codimensions. But the universal form for the codimension function (or equivalently the structure function exponent) was not known then.

Later, in Schertzer & Lovejoy (1987), they derive a universal form[17] for the codimension function which is dependent on just two parameters, α and C_1 (the "codimension of the mean"),

$$c(\gamma) = C_1\left(\frac{\gamma}{\alpha' C_1} + \frac{1}{\alpha}\right)^{\alpha'} \quad (\text{for } \alpha \neq 1)$$

where $\frac{1}{\alpha} + \frac{1}{\alpha'} = 1$ (and this α bears no relationship to the α of the α-model). Their model, the "continuous cascade model," is based on the use of exponentiated Lévy[18] random variables (r.v. for short) which have the property of stability under multiplication (to be described in detail in chapter II). As applied to turbulence the codimension may be converted using a Legendre transform (Parisi & Frisch 1985) to a structure function exponent and in this case the universal form becomes

$$\zeta(q) = \tfrac{1}{3}q - \frac{C_1}{\alpha - 1}\left((\tfrac{1}{3}q)^{\alpha} - \tfrac{1}{3}q\right). \qquad (I.11)$$

A number of other cascade models have also been proposed by various researchers which have different properties; a few of the major models still competing for attention in the current literature are the "random β-model" (Benzi et al. 1984), the "p-model" (Meneveau & Sreenivasan 1987) and the "She-Leveque model"[19] (She & Leveque 1994). For a

comparison of the predicted $\zeta(q)$ functions for various models with data see Anselmet (1984), Leveque & She (1997) and Schertzer et al. (1997).

Fig. I.10: Paul P. Lévy (picture from O'Connor & Robertson 1999)

But these cascade models were designed more with statistics in mind than the production of life-like representations of naturally occurring events; a visualization of the generated field to be compared with a recording of the natural one is not usually provided. Apart from arguments based on fundamental points of the theory their testing ground is simply the form of $\zeta(q)$. But that does not mean that simulation is not possible, especially since these models do produce an actual field as opposed to just some statistical quantities. The continuous cascade model is a good example of a model that has been used to simulate a wide variety of geophysical fields. Nevertheless it should be noted that the applicability of these models to any 'random' data or field has been restricted to the simplest possible case, namely to fields of positive valued quantities only, such as the energy flux or absolute value of velocity increments for which they were originally developed. This puts these models at a strong disadvantage when compared with direct numerical simulation (DNS) of the Navier-Stokes equation for a (two or) three dimensional velocity field.

I.5 A More Realistic Model

An interesting innovation can be found in Ott et al. (1992) when they apply the idea of signed measures to multifractals. The result is the so-called "cancellation exponent" which, if greater than zero, indicates an oscillation in sign at arbitrarily small scales. This notion is later taken up by Vainshtein & Sreenivasan (1994) in a theory of the oscillation in sign of the velocity field in fully developed turbulence. Yet despite this work there is not yet a model (in the sense that it may simulate an 'observable' field) of turbulence based on this idea. Furthermore it is still limited to scalar quantities.

Another 'extension' which is similar, in that it deals with a mathematical idea of multifractals rather than create an explicit model, is found in Riedi & Scheuring (1997). They note that in nature there are usually related components (variables) of a system whose interaction with each other is of great interest. Their "conditional multifractal spectrum" provides information about the relation between two distributions and goes beyond a simple correlation in that it involves moments of all orders. But this may find its usefulness in analysis rather than simulation.

Of a more dynamic nature, yet quite different to the models discussed so far, are the so-called shell models. Almost as if governed by the Navier-Stokes equation these model the time evolution of the 'generalized velocity' at discrete, geometrically spaced intervals (cells) in scale. As such they ultimately can only provide a statistical result for the energy and enstrophy of the turbulence they model. One of the first shell models, by Gledzer (1973), in two dimensions has been extended to three dimensions by Yamada & Ohkitani (1987) by introducing a complex quantity for the generalized velocity (called the "GOY shell model"). They found that their model exhibits good power law scaling which follows the Kolmogorov-Oboukhov five-thirds law. But as a model with only a single cell at each resolution, hence named one-path, it clearly departs significantly from being totally realistic.

Unlike the traditional shell models there is the "scaling gyroscopes cascade" (SGC) model of Chigirinskaya & Schertzer (1996). This deterministic shell model simulates the time evolution of the velocity vector and vorticity field in a 'tree structure' where the

number of model cells increases with the inverse of the scale. It has been run to simulate very large Reynolds number ($\approx 6 \times 10^7$) turbulence in both two and three dimensional configurations and was found to produce power spectrum scaling in close agreement with the Kolmogorov-Obukhouv result (see Schertzer et al. (1997) for these results) suggesting that it provides a reasonable model of the Navier-Stokes equation. The significant advantage of this model is that it contains an appropriate number of cells at the highest resolution and a velocity vector in each of these. This already provides a great deal more information about the system than the much more limited one-path shell models of generalized velocity. However the connection between cells in 'scale space' and real space has not yet been specified.

Motivated to go beyond scalar cascade modeling, Schertzer & Lovejoy (1995) have developed a general framework called "Lie cascades" which describes a multiplicative process for vectorial (and tensorial) fields[20]. The components of the vector represent the various variables of the system (also called "state variables") and are a natural way of providing a mathematical basis for multiplicative cascades which permit non-trivial interactions between these variables. The applicability of such an idea is not just limited to a turbulent velocity (vector) field, which is the most obvious example; any coupled processes may possibly be described by such a framework. As a concrete example they define an explicit cascade model for a field of two real variables which is called the "complex cascade model." By treating the azimuthal and radial components of the vector state as two independent universal multifractals they achieve a non-trivial mixing of the Cartesian components which represent the system. Note that now the state variables may take any real value, positive or negative. Hence this model is the most advanced in terms of providing a general model applicable to actual data.

I.6 Scope of the Thesis

Although the discussion so far has deliberately been kept narrowly focused on turbulence it is a fact that the ideas of scaling, or self-similarity, crop up in seemingly every field of science: the literature on this subject is already vast. Furthermore the applicability of the universal multifractal form (Schertzer & Lovejoy 1987) has been verified in many

different geophysical and other scaling fields (see Lovejoy & Schertzer (1995) for a review). It has been the aim in chapter I to provide a solid historical background for this model and some of the work by various researchers which point to its broad applicability. Having already done this the main subject of the thesis will not be to show the analysis of recorded data and comparison with the model. Rather the objective of this work is to clearly explain the model itself, to investigate how this knowledge may be used to simulate and analyse data, and how to overcome some of the difficulties in the latter. In § I.5 there is a brief review of extensions to the ancestor scalar models which leads to the more general Lie cascades.

Chapter II concerns itself with the details of the discrete universal multifractal cascade. The building material from which both the scalar and complex cascades are made is the Lévy r.v. whose properties are described in § II.2.3. Some examples of simulation are produced (§ II.4.1) and there is a brief discussion on the various analysis techniques available to the researcher (§ II.3). Of these just two are chosen for investigation in the subsequent § II.4.2. The attention to detail and care taken in producing the theory and results is necessary so that the work on complex cascades in chapter III may progress without any concern over elementary problems which would otherwise have arisen. This is the prerequisite to developing and testing the complex cascade analysis and simulation techniques of the following chapter.

Chapter III is very similar in structure to chapter II except that it deals with the complex cascade model (as already mentioned in § I.5). The rationale for choosing this model is that it is the most simple generalization of the well-understood scalar cascade which produces multivariate processes. The theoretical work of this chapter (§ III.2) closely follows the work of Schertzer & Lovejoy (1995). It shows in detail how the results have been derived, and in doing so some minor difficulties in the original work are eliminated. Following the explanation of the theory some simulations are produced in § III.3 and possible analysis techniques are described (§ III.4), including a new method called the "adjacent data points" (ADP) method (§ III.4.3). Having done so it is desirable to test these analysis methods on the simulations, and this is done in § III.5-6. It is found that the less trivial nature of the model leads to some complications (which are demonstrated

both theoretically and empirically) but the new analysis method is found to be an improvement over the conventional one. Some comments on the remaining difficulties of analysing recorded data are made in § III.7 (no analyses of recorded data are presented).

It was found to be well beyond the scope of this work to venture beyond complex cascades despite the lure of thrilling new discoveries. Indeed very little progress has been made towards establishing useful multivariate, universal multifractal models. Since (m.f.) universality is dependent on (r.v.) stability it is relevant to point out that in his foreword, written in 1981, Zolotarev (1983) states "I hope that the systematic exposition of the analytic properties of one-dimensional stable laws will stimulate analogous investigations for multidimensional stable laws, of whose properties very little is known to us." Still very little is known to us today.

Chapter I Notes

1 (The numbered footnotes in this chapter reference superfluous material which may be found here.) For more information on the hieratic city state the interested reader may consult eg., Campbell (1960), pp. 144-150.

2 Mikolaj Kopernik (a.k.a. Nicolaus Copernicus): b. Torun, Poland 19 February 1473; d. Frombork, Poland 24 May 1543

3 In a lecture delivered before the International Congress of Mathematicians in Paris in 1900 Hilbert spoke of his belief that there was no limit to the discoveries which could be achieved in mathematics: "This conviction of the solvability of every mathematical problem is a powerful incentive to the worker. We hear within us the perpetual call: There is the problem. Seek its solution. You can find it by pure reason, for in mathematics there is no *ignorabimus*." Hilbert (1900)

4 For a review on the nature of atmospheric turbulence and measurements thereof see Wyngaard (1991), or for a broad review of oceanic turbulence see Gargett (1989).

5 See eg., Lugt (1983) § 1.3 for some reproductions from Leonardo's work and discussion.

6 On the importance of Euler's findings in fluid dynamics Lagrange wrote "By this discovery, the entire mechanics of fluids was reduced to a single point of analysis, and if the equations which include it were integrable, one could determine completely the circumstances of motion and of action of a fluid moved by any forces. Unfortunately, they are so rebellious that up to the present time only a few very limited cases have been worked out." quoted in Truesdell (1968) p. 123

7 Andrei Nikolaevich Kolmogorov (walking in the Caucasus mountains): b. Tambov, Russia 25 April 1903; d. Moscow, Russia 20 October 1987

8 The exact third order longitudinal velocity structure function has been derived in Kolmogorov (1941b) giving $C_B = 4/5$ and is consequently known as the "four-fifths law." For a full mathematical account and an appraisal of Kolmogorov's 1941 turbulence theories see eg., Frisch (1995) ch. 6.

9 A fuller review may be found in Sreenivasan & Antonia (1997) § 3.3.1.

10 For a review covering the basic issues mentioned in this section the reader is directed to the excellent review by Sreenivasan & Antonia (1997).

11 Lewis Fry Richardson: b. Newcastle-upon-Tyne, England 11 October 1881; d. Kilmun, Scotland 30 September 1953

12 For a review on the application of fractals to turbulent phenomena see Sreenivasan (1991).

13 An interesting hybrid consisting of a multifractal on a fractal support may be found in Desaulniers-Soucy & Iuoras (1999).

14 NB that this β is not the same as the β used for the spectral slope (§ II.4.2) or the skewness parameter (§ II.2.3); these are three very different β's.

15 It should be noted that of the models existing up to this point in time the log-normal model was the only one which produced a non-linear behaviour in the structure function exponent. However this model has various theoretical shortcomings and is not a serious contender in the literature, see eg., Frisch (1995) pp. 171-173.

16 namely the "similarity dimension," the "information dimension" and the "correlation dimension"

17 For a review on universality classes and issues see Schertzer et al. (1997).

18 Paul Pierre Lévy: b. Paris, France 15 September 1886; d. Paris, France 15 December 1971

19 although also called the "log-Poisson" model

20 A more refined mathematical result (on the statistics of the process) is being written in Schertzer & Lovejoy (1999) which makes the rather abstract, general theory more pragmatic.

II Scalar Universal Multifractals

II.1 Introduction

In § I.4.1 it was described how a phenomenological model which can concentrate the activity into successively smaller scales is required to provide a degree of realism in models of turbulence. The (conserved) quantity being modeled is the energy flux passing from larger to smaller scales. The multiplicative cascade model was discussed and a universal form for the statistical properties, due to Schertzer & Lovejoy (1987), was introduced. Here the physical quantity being modeled is not a concern as the applicability of such models to many geophysical and other scaling processes has been demonstrated by others (see eg., Lovejoy & Schertzer 1995). The fundamental structure of the model itself is the subject of this chapter.

In § II.2.1 the second characteristic function, which is the basic mathematical quantity used to deal with r.v.s, is related to the (more physical) codimension function. The critical order moment above which the characteristic function exhibits "divergence of moments" is also determined in §§ II.2.1-2 This is an important effect which limits the usefulness of data analysis techniques. In §§ II.2.3-4 the theoretical properties of Lévy random variables are described as well as the basic discrete universal m.f. (DCUM) simulation method. It is important to know the properties, both mathematically and empirically (on a plot), of Lévy r.v.s to gain a feeling for the problems which are encountered later on in chapter III. In § II.3 some results are presented on the universal m.f. forms for the codimension and second characteristic functions and the more common analysis techniques which are available for analysing (m.f.) data fields. The focus in chapter III will be on only two of these techniques.

Finally in § II.4 the Lévy r.v.s themselves are displayed and analysed (as a test of the integrity of the software as well as for edification) as well as the DCUM simulations. The discrete nature of the cascade process used to simulate the m.f. field will become evident, as well as some of the finer limitations of the software. Thus having covered in some detail the basic r.v.s used as the generator and the method used to generate a DCUM field, as well as for its analysis, it will (later) be possible to go confidently into a discussion on complex

cascades in chapter III. (It should be noted that the material on Lévy r.v.s and multifractals, all the material in this chapter, is well described in such books as Feller (1966), Zolotarev (1983), Samorodnitsky & Taqqu (1994), Janicki & Weron (1994) on the former and Schertzer & Lovejoy (1996) on the latter.)

II.2 Basic Theory

II.2.1 c(γ), K(q) and q_s

The most simple form of cascade model has discrete cascade steps as in Mandelbrot's (1974) weighted curdling model (§ I.4.1). It may be considered in general such that at each step there is a change in scale by a factor of λ_0. Consider a field of energy flux occupying a volume of size L^d in d-dimensional space. Then at a scale $l_n = L/\lambda_0^n$ the corresponding energy flux ε_n may be constructed by taking the product $\varepsilon_n(x_n) = \mu\varepsilon_n(x_n).\varepsilon_{n-1}(x_n)$. This process, starting from the lowest resolution, is repeated as many times as is necessary to reach the desired resolution. (See eg., figure I.7 in 2 dimensions where λ_0=2.)

The random multiplier $\mu\varepsilon_n$ is an independent realisation of a random variable, one realisation for each individual step in the cascade. Its probability distribution is dependent on the details of the particular model, and may be described by its second characteristic function K(q) (described later in § II.2.3) as in the expression $\langle \mu\varepsilon^q \rangle = \lambda_0^{K(q)}$. Since each step in the cascade is independent of the others then, at the resolution $\lambda = \lambda_0^n$, $\langle \varepsilon_\lambda^q \rangle = \langle \mu\varepsilon^q \rangle^n$. The important result is that for a self-similar multiplicative cascade

$$\langle \varepsilon_\lambda^q \rangle = \lambda^{K(q)}.$$

For a normalised cascade $K(1) = 0$ at all resolutions.

The field at a given point in the cascade, and at a given resolution, may be characterised by the order of singularity γ, given by

$$\varepsilon_\lambda = \lambda^\gamma.$$

A useful characterisation of the field is the codimension, $c(\gamma)$, which comes from the probability of exceedence $\Pr(\varepsilon_\lambda > \lambda^\gamma) = N/\lambda^d = \lambda^{-c(\gamma)}$ (eqn. I.9). If the codimension function for a given field is known then it is possible to estimate the largest observed singularity, γ_S, given N_S samples of the field. It may be expected that $N_S\lambda^d\lambda^{-c(\gamma_S)} \sim 1$ and hence $c(\gamma_S) \approx d + D_S$, where the "sampling dimension" is defined as $D_S = \log_e N_S/\log_e \lambda$.

In fact the codimension and the second characteristic function can be related by use of the Legendre transform (eg., Schertzer & Lovejoy (1995) pp. 55-57) giving

$$K(q) = \max_\gamma \{q\gamma - c(\gamma)\}. \tag{II.1}$$

Thus the singularity γ_S corresponds to the moment

$$q_s = \left.\frac{dc(\gamma)}{d\gamma}\right|_{\gamma_s}. \tag{II.2}$$

A limitation which exists when evaluating the statistics of a field is that the largest singularity present will dominate the characteristic function for the large order moments. The result is a linear $K(q)$ function for q-order moments greater than a critical value q_s. (A similar limitation exists at the negative end of the distribution function as well.) This sort of effect, where the evaluated function diverges from the ideal, has been called a "phase transition," because of its similarity to the change in behaviour seen in thermodynamic quantities, or "divergence of moments."

II.2.2 Universality and stability

In general for a multifractal field the codimension function, or second characteristic function, can itself only be characterised by an infinity of parameters. However the idea that only several parameters will be relevant in a given process is usually very reasonable. Hence the notion that repeated iterations of a process with itself will converge towards a limit, and that by starting with somewhat different processes the same limit will also be reached (a stable attractor). For example, for a long time there has been the tacit assumption that multiplicative processes tend towards a lognormal distribution as an attractor. This convergence to a stable attractor is called universality.

It is more natural to work with the generators (a term taken from group theory) of the multiplicative process where universality implies that there will be stability of these exponents under addition (since multiplication results in the addition of exponents). The generator is written

$$\Gamma_\lambda = \log_e \varepsilon_\lambda .$$

Stability under addition has long been known in the form of the central limit theorem (giving rise to a normal distribution) and more generally in the form of the Lévy stable distribution. Therefore the use of a Lévy random variable as the generator will be investigated.

II.2.3 Lévy random variables

The random variable x is said to be "stable" (under addition) if it satisfies the condition

$$\sum_{i=1}^{n} x_i \overset{d}{=} a_n x_1 + b_n \text{ where in fact } a_n = n^{1/\alpha} \text{ and } 0 < \alpha \leq 2.$$

($\overset{d}{=}$ indicates equality in distribution.) Such a stable r.v., or "Lévy random variable," is characterized by just four parameters and (in the notation of Samorodnitsky & Taqqu (1994) or just S&T for short) is written

$$x \sim S_\alpha(\sigma, \beta, \mu)$$

where α is called the "Lévy index," σ the "scale parameter," β the "skewness parameter"* ($-1 \leq \beta \leq 1$) and μ is the "shift parameter." (When $\alpha = 2$ the resulting distribution is always symmetric about its mean and the skewness parameter loses its relevance: it is the Gaussian or "normal" distribution.) When $1 < \alpha \leq 2$ the shift parameter is also the mean. In the discussion below the mathematically special case when $\alpha = 1$ is omitted because it turns out that those distributions will not be used in this thesis.

---

* NB that this β is not the same as the β of the β-model (§ I.4.1) or the spectral slope (§ II.4.2)

The (Fourier) characteristic function of the random variable x is defined as

$$\left\langle e^{iqx} \right\rangle = \int_{-\infty}^{\infty} e^{iqx} p(x) \mathrm{d}x, \text{ for any real } q,$$

where $p(x)$ is the probability density function (p.d.f.) of x and the angle brackets, $\langle\ \rangle$, denote an integral over probability space. The second characteristic function is the logarithm of the characteristic function and for a Lévy r.v. is complex in general. It is given by

$$\log_e \left\langle e^{iqx} \right\rangle = -\sigma^\alpha |q|^\alpha \left(1 - i\beta (\operatorname{sign} q) \tan \frac{\pi\alpha}{2} \right) + i\mu q \qquad \text{(II.3)}$$

where $\operatorname{sign} q = \pm 1$ depending on the sign of q. This expression is only valid for $\alpha \neq 1$. But this is not the most practical quantity to work with: there is also the Laplace characteristic function for real $q \geq 0$,

$$Z(q) = \left\langle e^{qx} \right\rangle ,$$

and its logarithm which is the Laplace second characteristic function. This integral only converges if $\beta = -1$. Since a multifractal field with a converging $K(q)$ is required the Lévy r.v. to use in a cascade model must have $\beta = -1$. The distributions with this value of skewness parameter are called "totally skewed left" or "extremal."

The corresponding Laplace second characteristic function when $\beta = -1$ is given by

$$K(q) = \log_e Z(q) = -\frac{\sigma^\alpha q^\alpha}{\cos\left(\frac{\pi\alpha}{2}\right)} + \mu q \text{ for } q \geq 0 \text{ and } \alpha \neq 1. \qquad \text{(II.4)}$$

The normalisation that would be required for a "conservative" (the mean value of the field is the same at all scales) cascade can be achieved simply by setting μ such that $K(1) = 0$. The Laplace second characteristic function will often be called the "second characteristic function" or just $K(q)$ for short. The second characteristic function corresponds to the moment scaling function (as will be defined in § II.3) evaluated at a particular resolution.

The parameterisation which was used in equation (II.4) is an arbitrary choice; it may be changed to give the two forms of $K(q)$ (for $\beta = -1$, $\mu = 0$ and $\alpha \neq 1$) which are used in this thesis:

$$K(q) = \frac{C_1}{\alpha - 1} q^{\alpha} \\ = cq^{\alpha}$$

In some places it will be more convenient to work with the second of these two forms as the basic building block of the theory. The relationship between the two parameterisations is simply $C_1 = c(\alpha - 1)$.

II.2.4 The discrete cascade universal m.f. (DCUM)

The universal multifractal result (Schertzer & Lovejoy 1987), based on the consideration of a continuous cascade model utilising Lévy r.v.s. is that for an universal multifractal field

$$c(\gamma) = C_1\left(\frac{\gamma}{C_1\alpha'} + \frac{1}{\alpha}\right)^{\alpha'} \text{ when } \alpha \neq 1, \qquad \text{(II.5)}$$

and by Legendre transform this gives

$$K(q) = \frac{C_1}{\alpha - 1}(q^{\alpha} - q) \text{ for } \alpha \neq 1. \qquad \text{(II.6)}$$

where $1/\alpha' = 1 - 1/\alpha$. The physical significance of the parameter C_1 is that for a multifractal field it is the codimension of the mean. This may be seen by considering equation (II.1) for the mean $K(1) = 0$; the singularity corresponding to the mean of the process γ_1 is obtained by solving $\gamma_1 = c(\gamma_1)$ to give $\gamma_1 = C_1$. The importance of C_1 is that for a multifractal with $C_1 > d$ (the dimension of the embedding space) the mean will not converge and the multifractal will be very sparse.

Using eqn. (II.2) equation (II.5) for the codimension function implies that for an universal multifractal q_s is expected to be

$$q_s \approx \left(\frac{d + D_S}{C_1}\right)^{\frac{1}{\alpha}}.$$

An universal multifractal field may be simulated by a discrete cascade using Lévy random variables. Starting with the Lévy r.v. x, such that $\langle e^{qx} \rangle = e^{cq^\alpha}$, the generator $\zeta = u_0^{(1/\alpha)-1} x - c$ may be formed as a building block. The cascade is then produced by raising $\lambda_0 = e^{u_0}$ to ζ powers, an independent realisation each time, and using these numbers as the multiplicative factors for each cascade step. For simplicity, when generating the cascade by computer, each cascade step is chosen to be over a factor of two ie., $\lambda_n = 2$. Hence after n cascade steps the field has reached a resolution of $\lambda = 2^n$. The resulting characteristic function of the field is given by

$$\left\langle e^{nqu_0\zeta} \right\rangle = e^{nu_0 c(q^\alpha - q)}$$
$$= \lambda^{\frac{C_1}{\alpha-1}(q^\alpha - q)}$$

which is the same as the universal multifractal result (as in equation II.6). Note that the mean value of the field is equal to one at all scales; it is a normalised conservative process. Therefore this model produces a normalised, conservative, universal m.f. field with parameters α & C_1.

The cascade model which has just been described actually works with a rather artificial discrete, branching structure in the cascade. It may be expected that this will introduce some artificiality into the resulting simulations. (In fact the evidence of this will be seen in § II.4.2.) Despite this evaluating the statistics at the same discrete resolutions from which the cascade was constructed, which is the usual practice, will still yield the exact result just derived. Hence such a field will be called a discrete universal m.f. (DCUM) field and may be used without serious concern for this theoretical imperfection.

II.3 Data Analysis Techniques

Before embarking on simulation and analysis some important results are collected together in this section to provide a more complete picture of scalar cascades from the point of view of data analysis.

So far the discussion on multiplicative cascades has been kept to conservative processes for simplicity, that is processes for which the mean value of the field does not

change in value with scale. In general a cascade process will be non-conservative and this may simply be expressed by introducing an additional scaling parameter H, the "degree of non-conservation," such that

$$\langle \varepsilon_\lambda \rangle = \lambda^{-H}.$$

The corresponding spectral slope (defined in equation II.9) for a non-conservative field (in 1-D) is given by $\beta = 1 + 2H - K(2)$. Hence a field for which $H>0$ contains relatively little 'power' at the small scales (compared with the large scales) and this makes it more difficult to analyse. Lavallée (1991) has found empirically that fractional differentiation of the field (power law filtering) to compensate for the degree of non-conservation can correct for this effect such that the multifractal parameters of the process may still be accurately recovered.

Furthermore the special case $\alpha=1$ has been neglected. The complete and general universal forms for the codimension and second characteristic functions are:

$\alpha \neq 1$	$\alpha = 1$
$c(\gamma - H) = C_1 \left(\frac{\gamma}{C_1 \alpha'} + \frac{1}{\alpha} \right)^{\alpha'}$	$c(\gamma - H) = C_1 \exp\left(\frac{\gamma}{C_1} - 1 \right)$
$K(q) = qH + \frac{C_1}{\alpha - 1}(q^\alpha - q)$	$K(q) = qH + C_1 q \log_e(q)$

(II.7)

The data is usually recorded at a single resolution. The second characteristic function, much used by mathematicians, may be evaluated on the normalised data directly as a simple way of characterising the statistics. A curve fit on the graph of $K(q)$ gives the parameters α & C_1. The one drawback is that it does not provide any information about the structure (the relationship between points in space) of a field.

The moment scaling function $K(q)$ is a general form of the second characteristic function, as defined in the expression

$$Z(q) = \langle \varepsilon_\lambda^q \rangle \approx \lambda^{K(q)}, \tag{II.8}$$

which is evaluated on data whose resolution has artificially been reduced (degraded) in some way. The most simple way to reduce the resolution is by "dressing" (averaging by

spatial integration) the data which takes advantage of its self-similar properties. The resulting data is denoted "dressed" in contrast to the actual data which is called "bare." When dressed data is analysed this is called the "trace moments" analysis method (Schertzer & Lovejoy 1987). It has been shown that the resulting moment scaling function for the dressed data is identical to that for the bare data except that there is a statistical divergence, or phase transition, for moments exceeding a critical order q_D. The value of q_D may be estimated by solving the transcendental equation

$$d = \frac{K(q_D)}{q_D - 1}$$

where d is the dimension of embedding space. Since the trace moments method uses averaging it cannot recover the value of H from the field. The spectral slope must be used for that purpose.

The trace moments analysis method has been improved upon in the "double trace moments" (DTM) analysis method (Lavallée 1991). Like trace moments the analysis is performed on dressed data except here the data at the highest resolution is raised to an η power first, then normalised, and then dressed to the desired resolution prior to analysing the qth power. The resulting moment scaling function is a function of both powers (on the LHS) and is given by the simple expression

$$K(q,\eta) = \eta^{\alpha} K(q).$$

As with trace moments this analysis does not recover H because it relies on averaging to change the analysis scale. Its advantage over trace moments is that the field may be raised to an arbitrary power without affecting the recovery of α.

Perhaps the most simple and the closest to the original ideas of multifractality is the "probability distribution/multiple scaling" (PDMS) technique (eg., Seed 1989). This method involves simply evaluating the codimension function for the dressed data as a function of γ at various resolutions according to equation (I.10). A curve fit may be performed on the resulting graph of $c(\gamma)$ to find the universal m.f. parameters as per equations (II.7). The difficulty with implementing this analysis is that the values of the

codimension obtained for different values of λ are quite sensitive to the normalisation of the data set. For this reason this technique is not used if it can be avoided.

Another method which originates from the work motivated by turbulence is to use structure functions (§ I.3.2). Note that this method is not limited just to velocity increments; the structure function exponent $\zeta(q)$ may be defined in general for a field ε_λ by the equation

$$\left\langle \left| \varepsilon_\lambda(x + L/\lambda) - \varepsilon_\lambda(x) \right|^q \right\rangle \propto \lambda^{\zeta(q)}.$$

The general expression for the universal form in terms of the structure function exponent was given in equation (I.11), but more generally it may be written

$$\zeta(q) = qH - K(q)$$

where the dependence on H has been made explicit (the $K(q)$ here has no H term like eqn. II.6). Using structure functions has the advantage that the differences of data points are used thereby removing the arbitrary 'd.c. component', or offset, in the data. Also the H parameter is recovered by this technique as dressing is not used. The disadvantage of this technique is that the theoretical connection between $\zeta(q)$ and $K(q)$ is not trivial and still requires some clarification.

The structure functions method, PDMS and the DTM methods will not be used for analysis in this thesis because of their less trivial mathematical connection with the discrete cascade when compared with the simple second characteristic function and trace moments methods.

II.4 Lévy r.v.s and DCUM simulation and analysis

II.4.1 Lévy r.v. simulation and analysis

In this section some of the numerical and practical considerations of generating Lévy r.v.s are discussed. Only totally skewed left r.v.s with $\mu = 0$ are considered. The parameter values $\alpha = 1.5$ and C_1=0.05 are chosen as being typical of the values recovered from the analysis of geophysical data. For this choice q_D>100 for a 1-dimensional

multifractal field which indicates that no inherent limitation is expected in the recovered statistics from the dressed data (for the more modest order moments of $q<10$ which are used in this section).

Computer simulation of Lévy r.v.'s is easy to perform by taking a combination of two uniform distributions on (0,1) according to the equation developed in Chambers, Mallows & Stuck (1976). S&T conveniently provide a FORTRAN routine (pp. 46-49) for doing this. The routine was rewritten in C and the two mistakes in the coefficients were corrected before use. The random number generator which was chosen is the popular 'RAN3' pseudorandom number generator of Press et al.'s (1988) 'Numerical Recipes.' It was used with a slight modification to give numbers distributed on (0,1) (rather than [0,1]). (Note that all the computer programs used in this thesis were written in C at double-precision for simulation and analysis with the one exception of the power spectrum calculations which were performed in single-precision downgraded from double-precision. The fundamental simulation routines for Lévy r.v.s, scalar and complex DCUM fields can be found in the appendix.)

The result of a sample simulation of a Lévy r.v. with $\alpha = 1.5$ and $C_1=0.05$ is shown in figure II.1, on the left, (the first 512 values) with a plot of the second characteristic function as found from the data on the right (statistics points, theory line). The simulation was $2^{16}=65536$ data points long. The curve fit for all q gives $\alpha=1.504$ and $C_1=0.0509$. There is excellent agreement with the theory for the second characteristic function up to $q=4$, with marked deviation above $q\approx8$. For this single realisation the calculated value of $q_s\approx7.4$.

It is better to view the second characteristic function on a log-log plot, as in figure II.2 (statistics points, theory line). The plot below has been evaluated on 2^{16} data points. The straight line fit (over the range $q=0.1$ to 10) in the log-log plot gives $\alpha=1.487$ and $C_1=0.0502$. The agreement with theory looks good over the range $q=0.5$ to 10.

It can be seen in figure II.2 that the statistics determined from the computer simulation deviate from following the straight line expected value. This is most noticeable at the

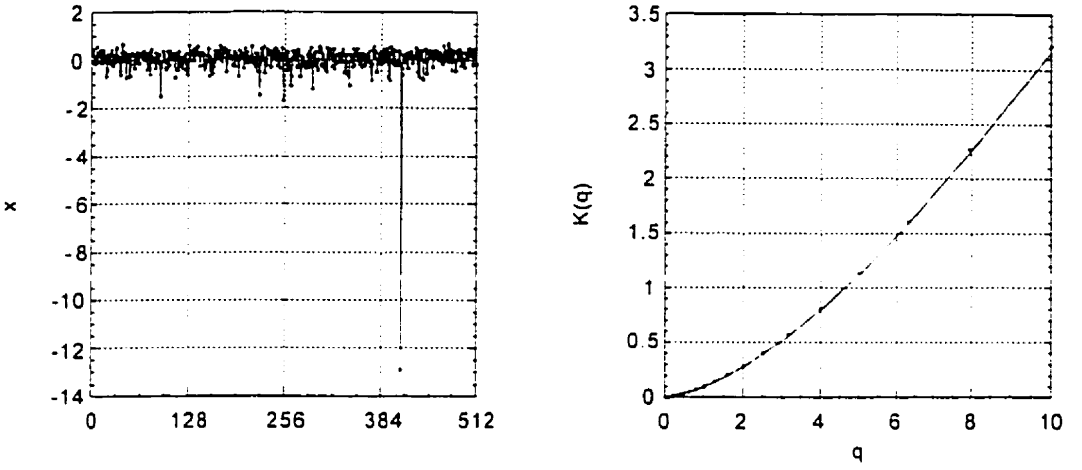

Figure II.1: 65536 independent realisations of a Lévy r.v. with $\alpha = 1.5$ and C_1=0.05 (left, part shown only) and its second characteristic function (right) as points with the theory line.

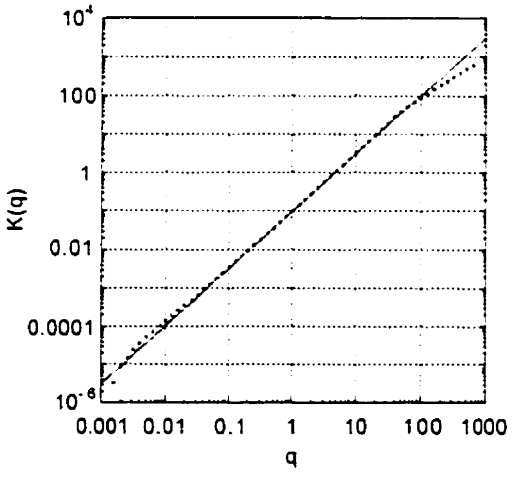

Figure II.2: Log-log plot of the second characteristic function in figure II.1.

small-q end of the graph, although this is seen at both large and small q. A deviation leading down and away from the straight line is mainly due to the finite sample size being used, any other deviation, especially a positive one above the line, can be attributed to an imperfect random number generator and/or small numerical errors in computation.

The Lévy r.v. itself has a certain probability density function (which has been chosen centred about zero). Once again with α=1.5 and C_1=0.05 a histogram of the data (2^{14} points) can be seen in figure II.3. The maximum and minimum values are -140.4 and 0.9717, respectively. The outliers at each end of the distribution (omitting end points) are -42.86, -31.85, -31.30, -22.26, -18.27 and 0.8261, 0.7963, 0.7715. There are only 41 data points with values less than -5, 1 with a value less than -50. There are 17 data points with values greater than 0.7. The mean of the data points is 0.0047 (cf. theory which gives zero).

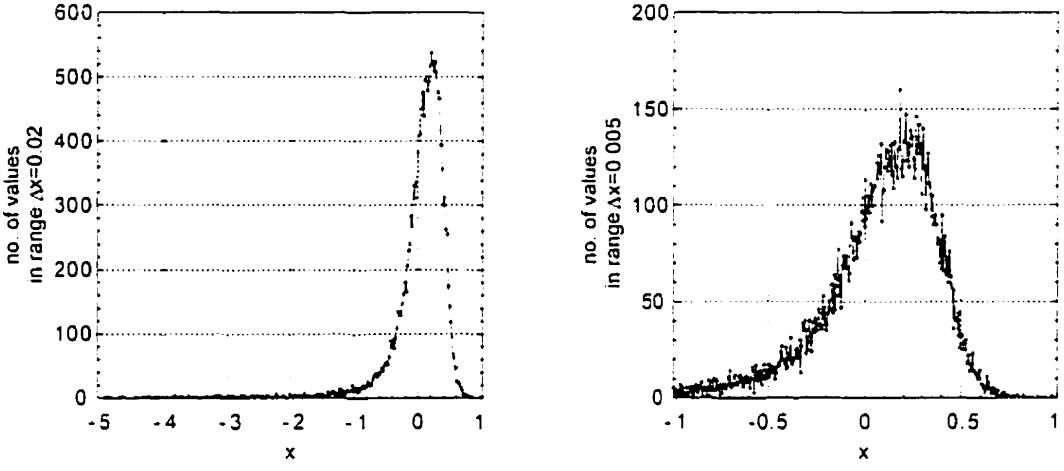

Figure II.3: Histogram of 2^{14} independent realisations of a Lévy r.v. with $\alpha = 1.5$ and C_1=0.05.

The probability densities of Lévy r.v.'s are continuous but are not known in a simple form (except for some special cases). The form for the rapid decay of the long and short tails at each end of the density function are (most clearly) given in S&T. Note that it is these low probability large positive/negative excursions (the positive ones forming singularities in the cascade) which are very important to the statistics at large/small order moments. (For a theoretical discussion on the probability density functions it is possible to consult Zolotarev (1983) §§2.4-2.7 for an exhaustive treatment.)

Exponentiating the r.v. (the generator, 1024 data points) gives the field on the left in figure II.4 (only first 512 points shown). The data values are uncorrelated with each other

and hence this field will exhibit a flat power spectrum. The actual power spectrum is shown on the right; it exhibits the noise (circles) which is typically seen in the statistics of a single realisation. An average over 1024 realisations (squares) shows a much less noisy result.

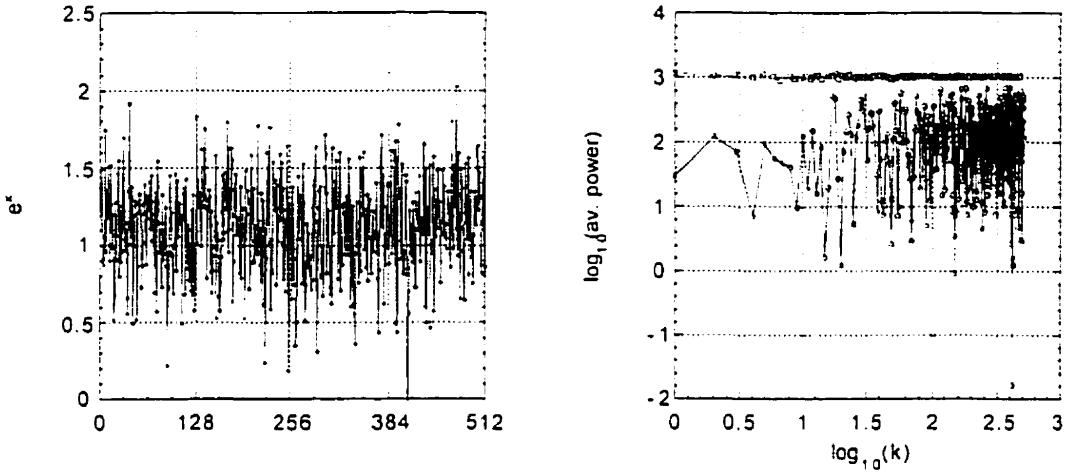

Figure II.4: Exponentiated Lévy r.v. (left), 512 data points, and its power spectrum (right) calculated on 1024 data points—one realisation (circles) and 1024 realisations (squares).

II.4.2 DCUM simulation and analysis

Scaling behaviour in a power spectrum takes the form

$$S(k) \propto k^{-\beta} \tag{II.9}$$

where β (*) is the "spectral slope." In a cascade simulation the spectral slope reflects the correlations between data points at a given resolution which exist because of the common ancestry which close data points will have due to the branching structure of the cascade. For a conservative cascade the spectral slope is given by $\beta = 1 - K(2)$ (see eg., Schertzer & Lovejoy (1996)) ie., the power spectrum is related to the second order moment statistics of

* NB that this β is not the same as the β of the β-model (§ I.4.1) or the skewness parameter (§ II.2.3)

the field. Hence for an universal multifractal field, where $K(2) = \frac{C_1}{\alpha-1}(2^\alpha - 2)$, the spectral slope will be given by

$$\beta = 1 - \frac{C_1}{\alpha - 1}(2^\alpha - 2).$$

It is worth noting that when C_1 is small β will be close to, and slightly smaller than, 1 (for a conservative cascade).

A DCUM simulation was constructed from scalar Lévy r.v.'s with α=1.5, C_1=0.05 with 16 levels giving a final resolution of 2^{16} data points. In figure II.5 the average power spectrum calculated for 2^{10} realisations may be seen. Note that the power spectrum data is averaged in logarithmic bins meaning that random fluctuations in the plot for higher values of k will be diminished. Clearly defined bumps can be seen in the spectrum (for large k) corresponding to the binary branching structure of the cascade. The theoretical slope is superimposed as a straight line over the statistics shown as points. The straight line fit for values with $\log_{10} k \geq 2.5$ gives a spectral slope of β=0.991 compared to the predicted value of β=0.917 ($\beta = 1 - K(2)$ where K(2)=0.083). The reason for this small discrepancy is not known.

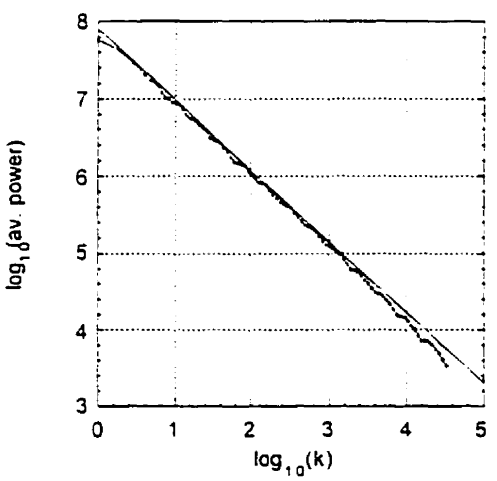

Figure II.5: Power spectrum of 2^{10} realisations of a DCUM simulation with $\lambda = 2^{16}$ and α=1.5, C_1=0.05.

The scaling behaviour is also evident in the plots of $\log_{10} Z_\lambda(q)$ (as defined in eqn. (II.8)) versus $\log_e \lambda$ evaluated on the dressed data (trace moments technique) for different values of q (=1, 2, 3, 4, 5 & 6) in figure II.6 (left), and the K(q) curve resulting from a straight line fit to these plots (shown on the right). (Statistics shown as points and the theory as lines in both cases.) The fit to the second characteristic function up to a value of q=6 gives α=1.469 and C_1=0.0502. These results are for 1024 realisations of 2^{16} data points. The slopes of the plots of $Z_\lambda(q)$ do not look so different to the theoretical slopes, though the statistics lie much closer to the theoretical line for smaller values of q.

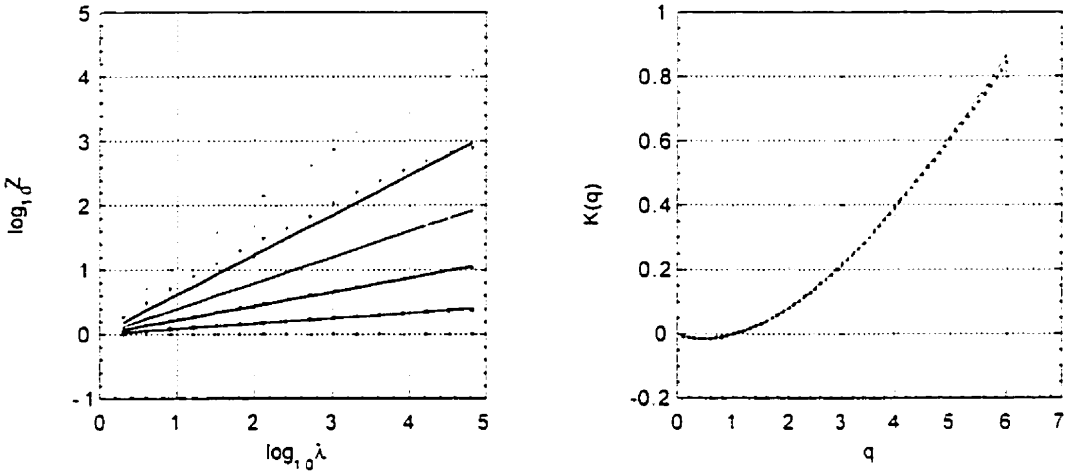

Figure II.6: Plots of $\log_{10} Z_\lambda(q)$ for q=1, 2, 3, 4, 5 & 6 evaluated by trace moments (left), and K(q) (right) from the straight line fits, evaluated on the same data as fig. II.5.

The scaling (fig. II.6) for higher values of q is a little suspect so the same graphs have been replotted up to q=2 in figure II.7 (scaling graph for q=0.5, 1.0, 1.5 & 2.0). The K(q) plot now gives the much more convincing fit with values of α=1.496 and C_1=0.0491. The statistics in this plot agree well with the theory over the approximate range q=0.5 to 1.5. This demonstrates that for the simulations being used the higher order moments should be used with some reservation.

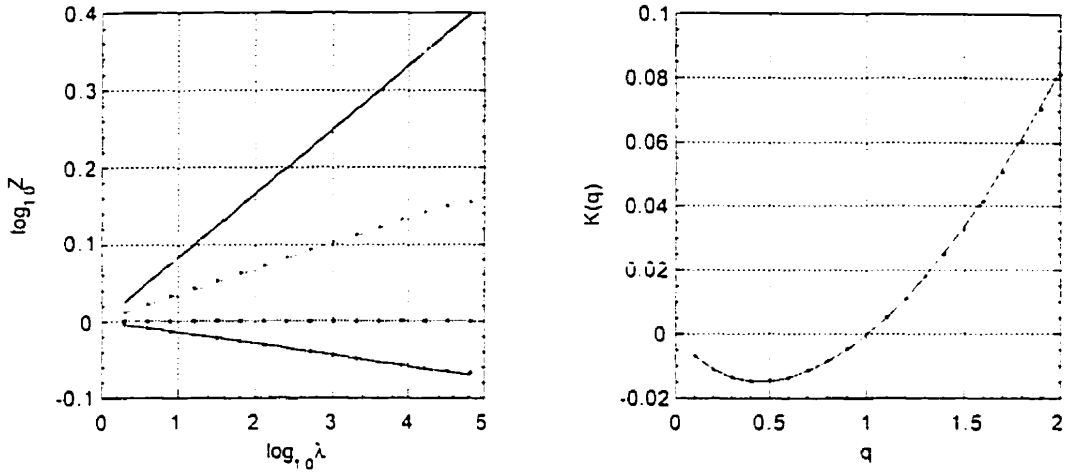

Figure II.7: Same as fig. II.6 but with different axes, for q=0.5, 1.0, 1.5 & 2.0 (left) as evaluated by trace moments.

The data at the highest resolution which has been created now looks quite different to the exponentiated Lévy r.v., as can be seen in figure II.8 (first 256 of 1024 data points). Note that the binary branching nature of the construction process can be seen in the field.

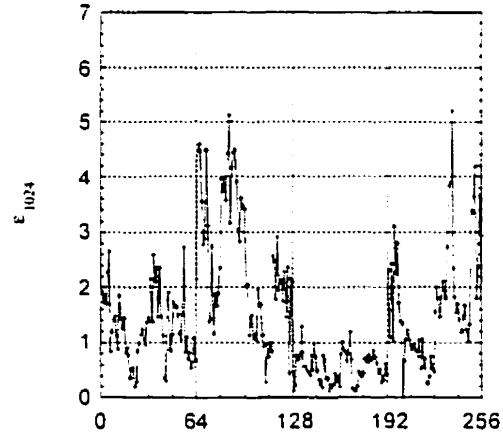

Figure II.8: Simulated field from a DCUM simulation with 1024 data points, 256 shown. The binary branching structure of the cascade can be seen in the data. $\lambda=2^{10}$ and α=1.5, C_1=0.05.

II.4.3 Concluding remarks on the simulations and analyses

The empirical characteristics of a Lévy random variable have been shown in § II.4.1 In particular the behaviour of the 'tails' in the p.d.f. have been described. For simplicity the simulations considered in § II.4.2 are only for conservative quantities. The discrete simulation method used produces fields which exhibit distinctive patterns from the binary branching structure of the cascade. This has not affected the statistics adversely as they have been evaluated at the same discrete resolutions present in the cascade itself. There are also some small and insignificant discrepancies between the statistics and the theoretical predictions which are due to the limitations of the software. The analysis of the DCUM field has shown that what can look like an apparently good line fit to the $K(q)$ function can be misleading as the parameters recovered in this way may be in error if the higher order moments are used. Thus it is best to utilise the lower order moments exclusively. All this knowledge will be of some use in chapter III.

III Discrete Complex Cascades

III.1 Introduction

Two variables in a field, which interact in some way, may be expected to display a form of correlated behaviour. The simple scalar, positive-valued models (of only a single field) in § I.4 are completely unable to describe such a system. Motivated with the desire to produce non-trivial fields some models were briefly described in § I.5 which could simulate the behaviour of natural physical fields more realistically, some of them even being multivariate. Apart from being capable of producing a field of signed numbers (with both positive and negative values) a rather general model which may produce a random vector field was among them ie., the Lie cascades model. (To describe the precise details of this model would be beyond the scope of this thesis, but the curious reader is directed to Schertzer & Lovejoy (1995) (to be denoted S&L for short) and Schertzer & Lovejoy (1999) for details.)

As a simple and practical example of the Lie cascades model S&L developed the theory for the "complex cascade" model (in § 3.2 of their paper) as well as showing the results of a simulation and some analysis of recorded data. The aim of this chapter is to make clear the theory behind this model, to show simulations and discuss in some detail the practical points of data analysis. This work (§ III.2) will closely follow the theoretical work in their paper but the simulation and analysis here (§§ III.3-6) is original.

S&L make the natural decision to represent two variables (at a point) as the real and imaginary parts of (a single) complex number. This conveniently ties the variables together and potentially allows various mathematical functions, which admit complex operands, to act in such a way as to mix the components together or keep them independent, as the case may be. In particular they consider the extension of the scalar random multiplicative cascade to the complex case by introducing independent r.v.s as the real and imaginary generators of the process. This is an arbitrary choice which imposes certain restrictions on the possible ways in which the two variables may be statistically related to each other. The reason for such a choice is the resulting relative simplicity in the mathematics. The complex

second characteristic function of the these complex random variables is the subject of § III.2.1.

Furthermore they give, as an example, the universal model which is derived by introducing Lévy r.v.s as the independent real and imaginary parts of the complex generator. Once again it should be stressed that there is no physical justification for this particular form, it is an arbitrary choice which may or may not be found representative of reality by subsequent testing on actual recorded data. (This latter aspect will not be a consideration here because of the difficulties encountered when doing so, as discussed in § III.7.) The universal complex result, as derived in § III.2.2, makes sense because scalar fields (almost always part of a multivariate process) are very often found to exhibit universality. Although derived from basics the universal result (in § III.2.2) has been obtained by closely following S&L. (It should be noted that some typographic errors are present in S&L's paper and that care has been taken not to allow these to contaminate the present work.)

Following the exposition of the basic theory some simulations of the resulting fields and variables are produced in § III.3. The usefulness of these simulations goes beyond testing the integrity of the software: the simulations are then analysed (in §§ III.5-6) with the aim of investigating the limitations of the analysis techniques themselves. Moreover it is found that the limitations of the analysis which are discovered may be understood by a study of the basic properties of the simulations in the first place. In fact the fundamental difficulty which will be encountered in the analysis arises because some functions of complex numbers do not give single valued results. Of these functions the logarithm and the fractional power are of concern (eg., there are three cube roots of eight, one real and two complex). This, coupled with the limitations imposed by the limited sample size and number of realisations, is found to curtail the usefulness of the analysis techniques being used. The analysis techniques themselves are described in § III.4.

III.2 Complex Cascade Theory

III.2.1 Complex K(q)

A mathematical way of dealing with two variables simultaneously is to treat them as the real and imaginary parts of a single complex number. When this is done a multiplicative complex cascade may easily be generated by choosing complex random variables as multipliers. Hence there is a corresponding complex order of singularity, or generator, defined by the equation

$z_\lambda = \lambda^{\gamma_R + i\gamma_I}$ where γ_R & γ_I are real.

The moment scaling function for the complex cascade is, in general, a complex quantity (ie., a complex function of a real variable). The moment scaling equation is

$\langle z_\lambda^q \rangle = \lambda^{K(q)}$ for real q.

Note that the above integral over probability space may not converge for some values of q depending on the characteristics of z_λ. Normalisation of the (conservative) cascade requires that $K(1) = 0$ at all resolutions.

The moment scaling function may be evaluated separately on the real and imaginary singularities making up the complex field. These are found by evaluating (the RHS's of)

$$\lambda^{K_R(q)} = Z_R(q) = \left\langle |z_\lambda|^q \right\rangle \text{ and } \lambda^{K_I(q)} = Z_I(q) = \left\langle \left(\frac{z_\lambda}{|z_\lambda|} \right)^q \right\rangle. \qquad \text{(III.1)}$$

Note that $K_R(q)$ is real whereas in general $K_I(q)$ is complex. The significance of these two exponents is that they represent the characteristics of the random variables responsible for i) modifying the magnitude or radial component of the complex quantity (without mixing the real and imaginary parts) and ii) modifying the rotational or azimuthal component of the complex quantity or, in other words, transferring 'intensity' from one component to the other.

If the real and imaginary parts of the generator are independent then

$$K(q) = K_R(q) + K_I(q). \qquad \text{(III.2)}$$

Coupled with the condition of normalisation this implies that for a normalised conservative field

$$K_R(1) + \mathrm{Re}\,K_I(1) = 0 \;\&\; \mathrm{Im}\,K_I(1) = 0 \text{ ie.,}$$

$$K_R(1) = -\mathrm{Re}\,K_I(1) \text{ and } K_I(1) \text{ is real.} \qquad \text{(III.3)}$$

III.2.2 Complex universality

As in the scalar case stability under addition in the generator of the process may be sought. Consider the outcome of choosing independent Lévy r.v.s for the real and imaginary parts of the complex generator. It may be recalled from equations (II.2-3) that the second characteristic functions for two independent Lévy r.v.s with equal scale parameters, expressed here in the codimension parameterisation $C_{1,R}$ & $C_{1,I}$, are

$$K_R(q) = \log_e\left\langle e^{iq\gamma_R}\right\rangle = \frac{C_{1,R}}{\alpha_R - 1} q^{\alpha_R} + \mu_R q \text{ and}$$

$$K_I(q) = \log_e\left\langle e^{iq\gamma_I}\right\rangle = \frac{C_{1,I}}{\alpha_I - 1}|q|^{\alpha_I}\left(\cos\frac{\pi\alpha_I}{2} - i\beta(\mathrm{sign}\,q)\sin\frac{\pi\alpha_I}{2}\right) + i\mu_I q. \qquad \text{(III.4)}$$

both for $\alpha \neq 1$. (Note that $\cos\frac{\pi\alpha}{2} < 0$ for $1 < \alpha < 2$.) These combine, as in eqn. (III.2), to create the total complex second characteristic function of the complex r.v. $\gamma_R + i\gamma_I$.

If both γ_R and γ_I are totally skewed left (β=-1) then the interchange of variables $\gamma_R + i\gamma_I \rightarrow \gamma_I + i\gamma_R$ in eqn.s (III.4) results only in a corresponding interchange of indices $I \leftrightarrow R$ in the second characteristic functions. This kind of symmetry between the real and imaginary generators would seem natural because mixing between the radial and azimuthal components of the complex field is a desirable feature of the complex model. This marks a departure from the mismatched codimensions of the mean in S&L which differ by a factor of $[\Gamma(3-\alpha_I)]/\alpha_I$. This is simply a feature of using different parameterisations. (It should also be noted that $K_I(q)$ (eqn. III.4) does not permit a real linear term in q. This is consistent with the result in equations (20) of S&L when considered in conjunction with their equations (19).) Of the Lévy r.v.s themselves γ_R is still required to be totally skewed

left (β=-1) to assure convergence of the integral whereas this restriction is now lifted from γ_I. Thanks to this convergence condition on $K_R(q)$ it is convenient to only consider the case q>0.

Imposing the conditions for normalisation (eqn. III.3) it is found that the shift parameters must be

$$\mu_R = -\frac{C_{1,R}}{\alpha_R - 1} - \frac{C_{1,I}}{\alpha_I - 1}\cos\frac{\pi\alpha_I}{2} \text{ and}$$

$$\mu_I = \beta\frac{C_{1,I}}{\alpha_I - 1}\sin\frac{\pi\alpha_I}{2}$$

hence the expected universal result for a normalised complex cascade is that for q>0

$$K_R(q) = \frac{C_{1,R}}{\alpha_R - 1}\left(q^{\alpha_R} - q\right) - \frac{C_{1,I}}{\alpha_I - 1}q\cos\frac{\pi\alpha_I}{2} \text{ and}$$

$$K_I(q) = \frac{C_{1,I}}{\alpha_I - 1}q^{\alpha_I}\cos\frac{\pi\alpha_I}{2} - i\beta\frac{C_{1,I}}{\alpha_I - 1}\left(q^{\alpha_I} - q\right)\sin\frac{\pi\alpha_I}{2}, \qquad \text{(III.5)}$$

both for $\alpha\neq$1. (Similar results for α=1 can easily be derived but these have been omitted here as they will not be used later on.) In particular it is found that under these conditions (normalised, q>0 & $\alpha\neq$1)

$$K_R(1) = -\frac{C_{1,I}}{\alpha_I - 1}\cos\frac{\pi\alpha_I}{2} \text{ and } K_I(1) = \frac{C_{1,I}}{\alpha_I - 1}\cos\frac{\pi\alpha_I}{2} \text{ (ie., } \mathrm{Im}\,K_I(1) = 0).$$

A word must be said about the interpretation of these new second characteristic functions. Whereas the quantity $C_{1,R}$ is known to be the codimension of the mean of the real part of the process there is no theory (at present) to say that the quantity $C_{1,I}$ in the second characteristic function is the codimension of the mean of the imaginary part. Thus if any interpretation of $C_{1,I}$ as being the codimension of the mean of the imaginary part of the process were to be made it would be purely speculative at this time. However, for the purpose of discussion, it will be assumed that the symmetry between real and imaginary generators implies that there is an effective codimension of the mean of the imaginary part.

III.3 Complex DCUM Simulation

The complex universal cascade simulation is performed in the same way as for the scalar simulations in chapter II. The difference here is that two independent realisations of the Lévy random variable are generated for each cascade step, these corresponding to the real and imaginary parts. The parameters for each r.v. are chosen independently and such that a normalised result is produced. The Lévy r.v for the imaginary generator is chosen to be totally skewed left.

Three sets of simulations are analysed in this chapter and they are characterised as in table III.1. The reason why $C_{1,I}$ for simulation B is not the same for simulation C is an arbitrary choice based on the fact that for these values of $C_{1,I}$ the values of $K_1(1)$ are equal (note that $\mathrm{Re}\,K_1(q) = K_1(1)|q|^{\alpha_I}$).

simulation	$C_{1,R}$	α_R	$C_{1,I}$	α_I
A	0.03	1.6	0.04206	1.8
B	0.03	1.6	0.4206	1.8
C	0.03	1.6	0.3536	1.5

Table III.1: Simulation parameters for chapter III

In each case the cascade is produced over ten steps of a factor of two down to a resolution of 1024, and the cascade starts from the large scale complex state $\varepsilon_1 = \frac{1}{\sqrt{2}}(1+i)$. (One realisation is being considered unless indicated otherwise.)

Figure III.1 shows plots of the real (left) and imaginary (right) components of complex simulation A. The imaginary component displays values of both positive and negative sign. This is a feature which cannot be observed in the discrete scalar cascades of chapter II.

Figure III.2 shows the scatter plots for simulation A (left) and B (right). The difference between the two is that the value of $C_{1,I}$ is ten times larger in simulation B (right). (The values are $C_{1,I}$=0.04206 in simulation A and $C_{1,I}$=0.4206 in simulation B.)

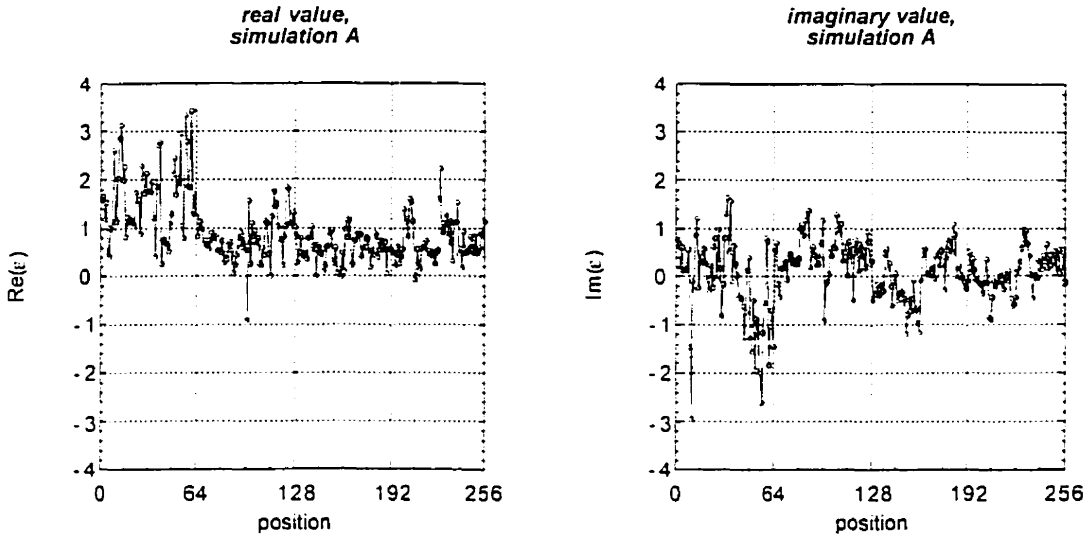

Figure III.1: plot of real (left) and imaginary (right) parts of complex simulation A. First 256 points shown.

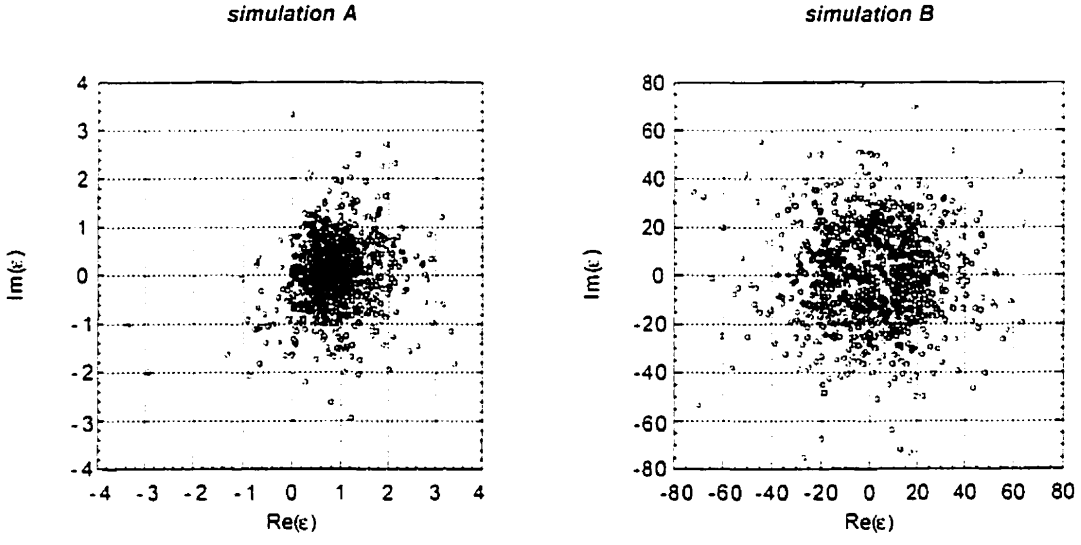

Figure III.2: scatter plots of complex simulation A (left) and B (right). Simulation B has a larger value of $C_{1,1}$ than simulation A.

For the plot on the left most of the points can be seen to cluster around the mean, but the more frequent negative outliers in the Lévy r.v.s produce two distinct tails; one rotating anti-clockwise and petering out as it does so (for outliers in the imaginary generator, γ_I), and the other producing a stem of points reaching down to the origin (for outliers in the real generator, γ_R). (The simultaneous occurrence of an outlier in γ_I and in γ_R is extremely

rare.) The plot on the right has an exaggerated rotational spread of the points due to the larger value of $C_{1,I}$. The values of $C_{1,I}$ in these simulations were picked so that simulation A would not contain many points with a large imaginary generator and so that, in contrast, simulations B & C would do.

The exponential of an imaginary quantity is a periodic function, hence for the complex state ε_λ there is a loss of information for those data points which have an imaginary exponent (argument of ε_λ) greater than $\pm\pi$: That is to say the inferred value of the imaginary exponent will only be its principal value. This loss of information occurs for the largest (imaginary) singularities, and for simulation A it will be a rare event whereas for simulations B & C (with larger values of $C_{1,I}$) it will occur more frequently.

The loss of information which occurs may have an adverse effect on the analysis of the data. An idea of what this does to the data may be seen by directly viewing the plot of the probability density of the argument, both actual (the generator in the simulation) and inferred (as inferred from the principal value of the argument of the complex data). Figure III.3 shows plots of the probability densities of the arguments of eight realisations of simulation A, the actual value (left) and the principal value (right). The plot of the actual value of the argument (left) shows the long negative tail and short positive one characteristic of a totally skewed left Lévy r.v.; the plot is asymmetrical. The positive singularities do not exceed a value of about 2.3. The difference in the plot on the right is that there are some extra data points with a value greater than 2.3. These are points from the negative tail which have been shifted to their principal value (and which happen to fall at around a value of $+\pi$).

Another related quantity whose statistics are of interest is the difference between two adjacent imaginary exponents. (This will be fully explained in the next section.) The plot in figure III.4 shows the probability density of the difference between two arguments as evaluated from the generator (line) and from the inferred argument values (points). Note that the plot is symmetrical and that the points calculated from the data values are necessarily restricted to the range $\pm\pi$. As with the right hand plot in figure III.3 the less

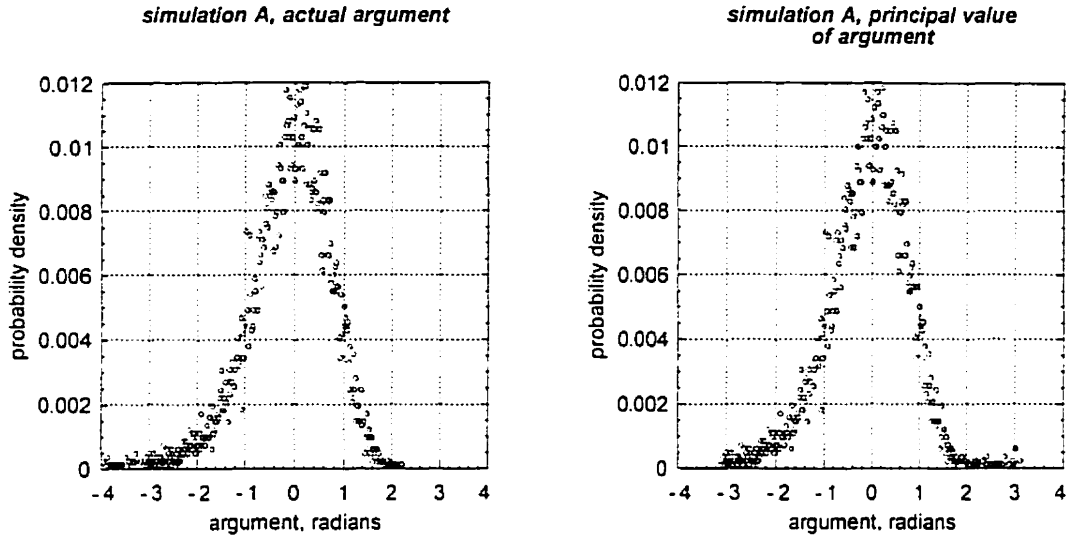

Figure III.3: Plot of probability density of the (true) argument of the bare data, left, and of the principal value of the argument, right, evaluated on 8 realisations of simulation A.

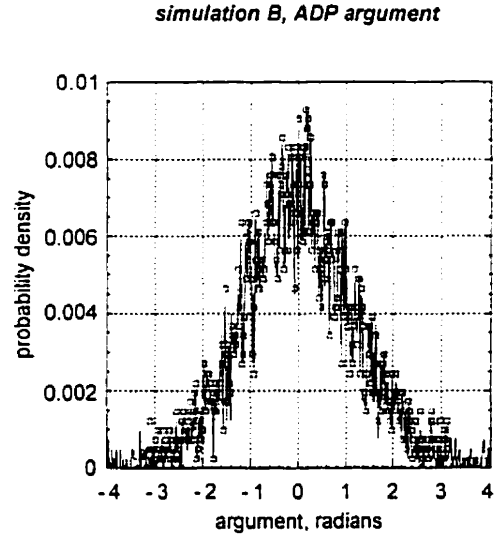

Figure III.4: Plots of probability density of the difference in arguments of adjacent data points for simulation B (8 realisations) as calculated from the imaginary generators (line) and the arguments inferred from the data (points).

frequent points near $\pm\pi$ are more frequent than they should be due to the loss of information.

The effect, on the analysis, of the shifted data points in the probability density seen in both figures III.3 (right) and III.4 will become apparent in the analysis section of this chapter.

III.4 Complex Analysis Techniques

III.4.1 Knowledge of the characteristic parameters

Analysis may be performed in a straightforward fashion by evaluating the quantities in equations (III.1) and comparing the real and imaginary parts of the moment scaling functions with the universal forms given by equations (III.5). In particular the quantities

$$\lambda^{K_R(q)} = Z_R(q) = \left\langle |z_\lambda|^q \right\rangle \text{ and } \lambda^{\mathrm{Re}K_I(q)} = Z_{IR}(q) = \left| \left\langle \left(\frac{z_\lambda}{|z_\lambda|} \right)^q \right\rangle \right|$$

(on the RHS's) are evaluated. The moment scaling functions for normalised z_λ may then be expressed explicitly in the convenient forms (III.6-8) below.

$$K_R(q) - q K_R(1) = \frac{C_{1,R}}{\alpha_R - 1}(q^{\alpha_R} - q) \qquad \text{(III.6)}$$

when the contribution from the 'mean' ($q K_R(1)$) has been subtracted. Quantitative knowledge of this mean quantity enables $K_I(1) = -K_R(1)$ (eqn. III.3) to be determined and hence the quantity

$$K_I(1) = \frac{C_{1,I}}{\alpha_I - 1}\cos\frac{\pi\alpha_I}{2} \qquad \text{(III.7)}$$

can be found from $Z_R(q)$. In fact this equation (III.7) is a special case of

$$\mathrm{Re}K_I(q) = \frac{C_{1,I}}{\alpha_I - 1}q^{\alpha_I}\cos\frac{\pi\alpha_I}{2}. \qquad \text{(III.8)}$$

All the statistical properties of the complex field z_λ are contained in equations (III.1). But it should be noted that the argument of the quantity $Z_I(q)$ has been kept out of equation (III.8). This is because the ambiguity in evaluating it, as discussed in § III.3 and later in

this chapter, makes it a very erratic quantity. A practical way of extracting useful data from this quantity has not been found. Therefore the characterisation which results from using only equations (III.6 & III.8) is not complete for any general complex field, although if the field is a universal complex m.f. all the statistical parameters required to define it may still be recovered (as is evident by all four parameters being present in those equations).

In summary the parameters which may be recovered from data analysis if only the function $Z_R(q)$ can be determined accurately are $K_I(1)$, $C_{1,R}$ & α_R; knowledge of $K_I(1)$ does not give any information about $C_{1,I}$ independently of α_I. (The quantity $K_I(1)$ in itself quantifies the effect the imaginary generator has on $K_R(q)$; it may have some greater physical significance but this is not known at this time.) Only if $Z_I(q)$ is known can $C_{1,I}$ & α_I be recovered from the data. If both $Z_R(q)$ and $Z_I(q)$ are known then there is a redundancy of the information of $C_{1,I}$ & α_I which may be used as a test for consistency.

III.4.2 The trace moments method

The trace moments method (§ II.3) for evaluating the statistics of a stochastic process is used to evaluate the moment scaling function of the data at different resolutions. Since the data is available only at a single resolution it is necessary to (repeatedly) dress the data to bring down the resolution for analysis. However, the bare and the dressed data are not the same thing; dressing the data alters its statistics (§ II.3). For a scalar process the statistics are the same up to the moment of order q_d (beyond which point they diverge) which means that provided q_d is large enough the trace moments analysis is very useful for recovering the true statistics of the data. Unfortunately at present there is no theory to determine what the critical moment for complex multifractals is.

For the complex case there may be an additional difference in behaviour between the statistics of the dressed and the bare data because of the loss of exponent information. Empirical observations, and comparison with theory, of the statistics evaluated by the complex trace moments method from dressed data will be made in the following sections.

III.4.3 The adjacent data points (ADP) method

The relationship between the complex field and the complex order of singularity may be defined by the equation

$$\varepsilon_\lambda = e^{\log_e \lambda(\gamma_R + i\gamma_I)} = e^{\Gamma_{R,\lambda} + i\Gamma_{I,\lambda}}.$$

It was already mentioned in the previous section that the imaginary exponent $\Gamma_{I,\lambda}$ cannot be known unambiguously from the complex data because there will be a loss of information if its value does not fall within the range $\pm\pi$; only the principal value of $\Gamma_{I,\lambda}$ can be known from the data. This will be a problem because taking a non-integer q-power of ε_λ will not give the same result as exponentiating q times the true exponent (unless the true value of $\Gamma_{I,\lambda}$ is the same as its principal value). There will be an error due to the difference between the two, and this error may be expected to deteriorate the quality of the calculated statistics in some way. To reduce this error it is possible to try reducing the size of the $\Gamma_{I,\lambda}$'s being dealt with.

When $C_{1,I}$ is large, and the effective size of the singularity is amplified by the $\log_e \lambda$ term at a high resolution, then $\Gamma_{I,\lambda}$ will be large. Hence by reducing the effective resolution it may be possible to reduce the size of $\Gamma_{I,\lambda}$. This may be achieved by considering the ratio of complex states adjacent in position (in the cascade) at the same resolution ie., consider a sub-cascade whose final resolution is two—it consists of just two data points (adjacent data points or ADPs) with the same common 'parent.'

Consider the characteristic function for the complex generator of one cascade step, $\zeta = \gamma_R + i\gamma_I$, in a sub-cascade of resolution 2 defined as $\left\langle 2^{q\zeta} \right\rangle = 2^{K(q)} = 2^{\mathrm{Re}K(q) + i\,\mathrm{Im}K(q)}$. Then the characteristic function of the ratio of the two independent steps (in the sub-cascade) is simply

$$Z_A(q) = \left\langle 2^{q(\zeta_1 - \zeta_2)} \right\rangle = 2^{2\,\mathrm{Re}K(q)}$$

as follows from equations (III.4). Note that the imaginary part of this characteristic function is zero, the statistics are symmetrical, and in terms of Lévy r.v.s β=0. (This implies that any attempt to evaluate the Laplace characteristic function would result in

divergence.) Hence this method is rather different to the other analysis methods (in this thesis) as it changes the statistics of the imaginary generator. Also the effective resolution of the new quantity whose statistics are being evaluated is 4 (and hence the subscript which is used). In a self-similar cascade this quantity is simply given by the ratio of ADPs

$$z_{4,(\lambda)} = \frac{\varepsilon_{i+1}}{\varepsilon_i}$$

where the indices i & $i+1$ indicate contiguity in space/time position. Here λ indicates the resolution at which the characteristic function is evaluated. It would be expected that the evaluated characteristic function will be independent of resolution only if dressing conserves the statistics.

(As an aside it is interesting to note that the ADP method may equally well be applied to a dressed or bare scalar field if pure imaginary powers of the ratios $z_{4,(\lambda)}$ are taken. The usefulness of doing this would have to be tested empirically. In some cases the advantages of this method may be found to outweigh the disadvantages of using it.)

The big advantage of analysing the statistics of ADPs (the ADP method) is that an analysis may be performed on data with an effective resolution of just 4 without the need to degrade its resolution. In this way the effective size of the imaginary singularities can be reduced without resorting to dressing complex data (with its unknown side effects). Another bonus of using this method is that since ratios of data values are used the field does not need to be normalised first. (This is advantageous if the correct normalisation of the field is not known eg., when it is difficult to recover the mean from the data.) Hence this method appears to be a viable alternative analysis method which should be tested alongside the conventional evaluation of the second characteristic function of the bare and dressed data. This is done in §§ III.5-6.

III.5 Conventional (Trace Moments) Analysis

The analyses in this section are on 1024 realisations of simulation A. Here the value of $C_{1,I}$ is small enough such that imaginary exponents outside the range $\pm\pi$ will be rare (in the bare data). These analyses will reveal how well the statistics may be recovered given the various limitations of numerical accuracy and the finite number of samples.

III.5.1 Small $C_{1,I}$

Figure III.5 shows the plots of Z_R (left) and Z_{IR} (right) evaluated from the data for q=0.5, 1, 1.5 & 2. In both plots the statistics (points) of the bare data (at the highest resolution) agree well with the theory (lines). Likewise the scaling in both plots (from the statistics of the dressed data) is good, as evidenced by the straight slope of the points. However these slopes do not correspond exactly with the theoretical ones, the discrepancy for Z_{IR} (right) being greater. This indicates that the dressing operation does not conserve the statistical properties of the bare data exactly (even for these relatively small values of q).

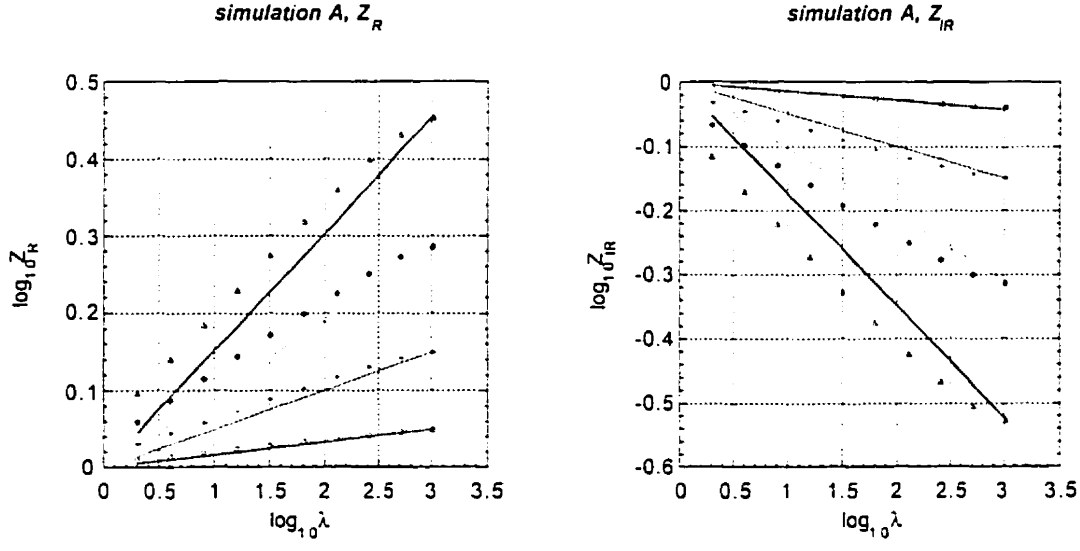

Figure III.5: Characteristic functions Z_R (left) and Z_{IR} (right) evaluated from 1024 realisations of simulation A for q=0.5, 1, 1.5 & 2. Theory lines, statistics points. Only the points at the highest resolution have been evaluated on bare data; the other points come from dressed data.

Next are the plots of the moment scaling function and second characteristic function in figure III.6. The plots of K_R, left, show that the statistics (circles) of the bare data agree very well with the theory (line) for q at least up to 6. The statistics (squares) from the dressed data give a reasonable agreement with the theory up to q=2. The plots of - $Re(K_I)$ (circles bare, squares dressed), right, show a reasonable agreement with the theory (line) in the approximate range q=0.5 to 4. Limitations due to the number of realisations begin to appear at the highest values of q in this plot. In both cases the statistics of the bare data agree well with the theoretical values, in the case of the dressed data the agreement gets worse as the order of moment of the statistics increases.

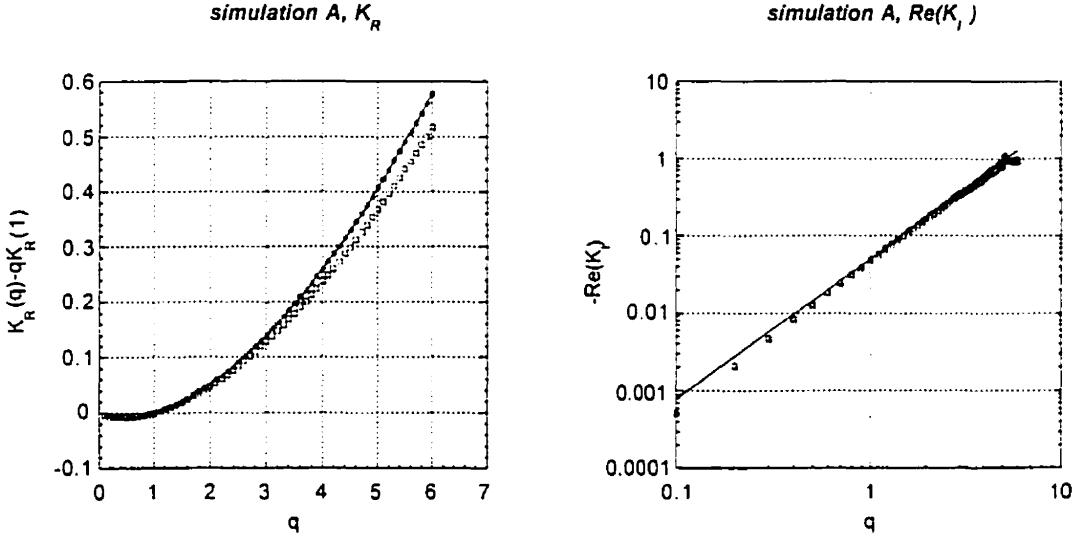

Figure III.6: Plots of moment scaling functions from K_R (left) and of $Re(K_I)$ (right). Statistics from the bare data (highest resolution) are squares and from the dressed data (from the slopes of trace moments) are circles. Lines represent theory.

In conclusion, it has been seen that the dressing operation does not exactly conserve the statistics of the process. This is especially true for the higher order moments where the effect is most pronounced. The evaluation of the statistics for K_R (when compared with the theoretical value) from bare data is excellent; for $Re(K_I)$ it is good for both bare and dressed data. These results represent the conclusion from analyses of simulations with a relatively small value of $C_{1,I}$.

III.5.2 Large $C_{1,I}$

The problem of having a relatively large imaginary exponent, that is when there is a large $C_{1,I}$, is now considered. Here 1024 realisations of simulations B & C (α_I=1.8 & 1.5 respectively) are analysed. These two simulations have a much larger value of $C_{1,I}$ than simulation A (in fact ten times larger).

Figure III.7 shows the plots for Z_R on the left and for Z_{IR} on the right for q=0.5, 1, 1.5 & 2 evaluated on simulation B. The plot for Z_R shows good scaling though once again the slopes of the (dressed) statistics do not agree with the slopes of the theory lines. The disparity between the dressed statistics and the theory is more pronounced here than it was for the smaller value of $C_{1,I}$ in simulation A. The statistics of the bare data continue to agree well with the theory.

The plot for Z_{IR} (right) shows two important defects i) the scaling is no longer good (and there is some 'randomness' associated with the statistics) and ii) the statistics for different values of q (=1 & 1.5) cross each other (which is incompatible with the theory). Here the bare statistics do not agree with the theory either.

The deterioration in quality of the dressed statistics (compared to the theory) which accompanies the increase in $C_{1,I}$ indicates that the dressing operation is not conserving the statistics due to the large size of the imaginary exponent and the corresponding loss of information in the data. The overall deterioration of the statistics of Z_{IR}, even when evaluated from the bare data, shows a complete failure of this particular analysis to reveal the true statistical character of the simulation. The corresponding $Re(K_I)$ plot may be expected to have some serious problems (fig. III.9 below).

The plot for K_R in figure III.8 shows that the bare statistics (circles) agree well with the theory (line) for all values of q shown. The statistics from the dressed data do not agree, even for small values of q. It may be concluded that the larger value of $C_{1,I}$ has affected the degraded data so much that the statistics for K_R no longer conform to the theoretical prediction. Hence to evaluate $K_I(1)$, $C_{1,R}$ & α_R only the bare data must be used, and then the analysis may still be expected to be fully accurate.

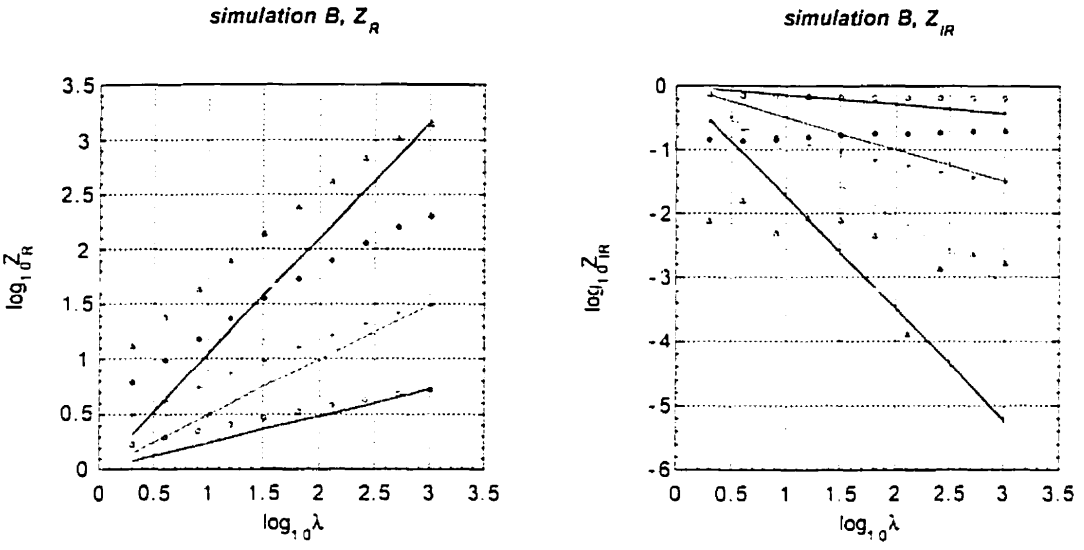

Figure III.7: Plots of Z_R and Z_{IR} for simulation B, 1024 realisations. In both plots q=0.5, 1, 1.5 & 2, theory lines, statistics points. The symbols for q=0.5, 1, 1.5 & 2 are circle, plus sign, diamond & triangle respectively.

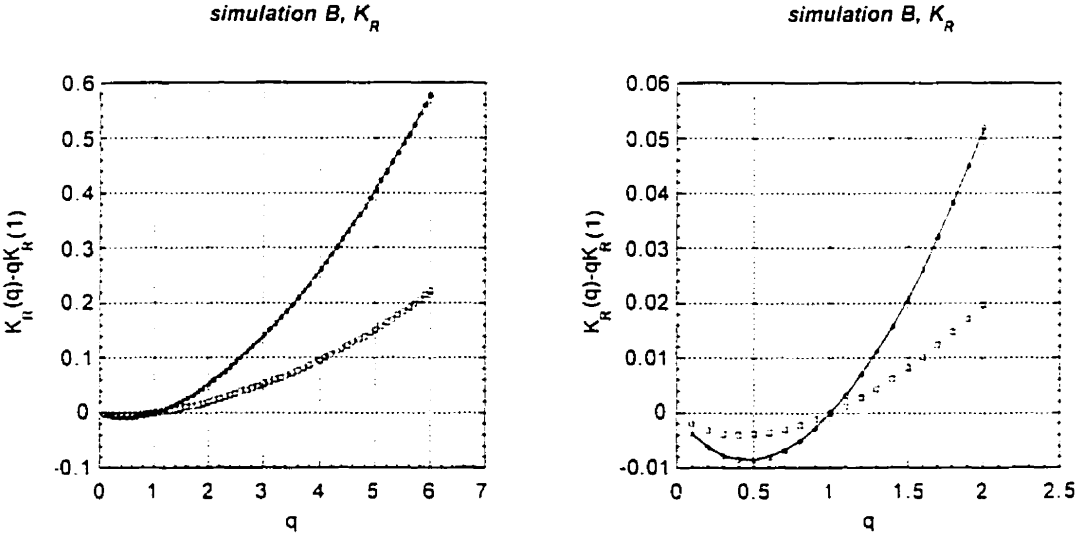

Figure III.8: Plots of K_R with different scales for the axes. Bare statistics represented by circles and dressed statistics by diamonds, theory line & statistics points.

Figure III.9 shows the plot for $Re(K_I)$ where the circles represent the bare statistics, diamonds the dressed statistics. Neither set of statistics agrees with the theory (line),

except for the single point $\mathrm{Re}\{K_I(1)\}$ evaluated on the bare data only. These results are not surprising given the defects seen in the plots of Z_{IR} (fig. III.7 above). There is also a periodicity in q, of one, which can be seen in the statistics. (This will be explained in the next section where this effect will be seen again.) Clearly this analysis is only of limited use.

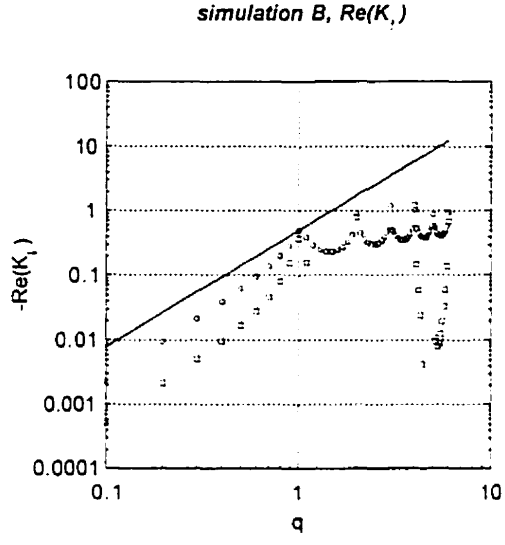

Figure III.9: Plot for $\mathrm{Re}(K_I)$, circles represent bare statistics, diamonds the dressed. Theory line, statistics points.

It may be concluded that the evaluated statistics of K_R remain very good for the bare data (only), which allows the accurate recovery of the values for $K_I(1)$, $C_{1,R}$ & α_R. Also that the value of $K_I(1)$ can still be recovered from the $\mathrm{Re}(K_I)$ statistics, but this only from the bare data. Hence for large values of $C_{1,I}$ the values of $C_{1,I}$ & α_i cannot be recovered using this method alone. This is a serious shortcoming.

III.6 Adjacent Data Points (ADP) Analysis

III.6.1 Small $C_{1,I}$

The statistics of $z_{4,(\lambda)}$ are now computed. Of the three statistical quantities which were calculated using the trace moments method (in § III.5) it is meaningful to evaluate just one using the ADP method, namely that of $Z_{4,IR}$. Here 1024 realisations of simulation A will be analysed.

The plot for $Z_{4,IR}$, figure III.10, shows that the statistics (points) of the degraded data differ significantly from those of the high resolution (not degraded) data. The theory (lines) are in close agreement with the highest resolution statistics only: As it has already been demonstrated (in § III.5) that degrading the simulated data changes the statistics in such a way as to adversely affect the complex analyses, degraded data will not be used for analysis in this section.

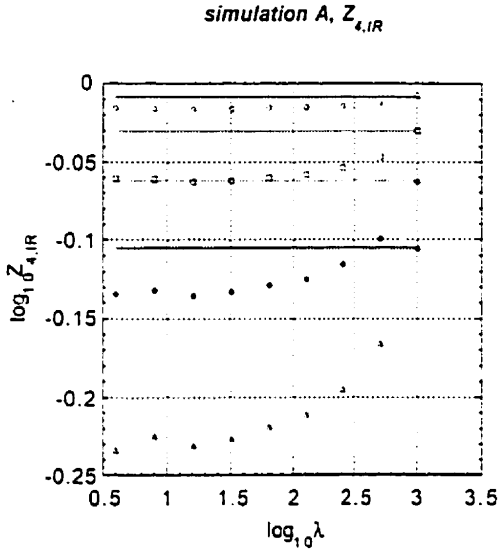

Figure III.10: Plot for $Z_{4,IR}$ for q=0.5, 1, 1.5 & 2, simulation A.

The plot for $\mathrm{Re}\{K_{4,I}\}$ at the highest resolution, figure III.11, shows that the agreement between theory (line) and the statistics (points) is very good for values of $q \geq 0.7$. For smaller values of q the slope becomes equal to 2.

The behaviour at small q may be thought of in terms of the series expansion of the integral for the characteristic function,

$$\begin{aligned} Z(q) &= \int_{-\infty}^{\infty} p(x) e^{iqx}\, dx \\ &= \int_{-\infty}^{\infty} p(x)\left\{1 + iqx - \frac{q^2x^2}{2!} + \ldots\right\} dx \end{aligned} \qquad \text{(III.9)}$$

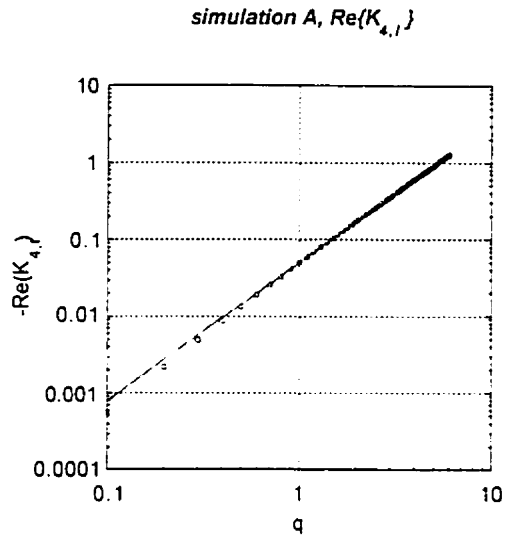

Figure III.11: Plot of $\mathrm{Re}\{K_{4,I}\}$ from the highest resolution data of simulation A. Theory line, statistics points.

It should be noted that using the ADP method results in a symmetrical p.d.f. Thus the odd moments in eqn. (III.9) all equate to zero giving

$$Z(q) = 1 - \frac{q^2}{2!}\int_{-\infty}^{\infty} p(x).x^2\,dx + \frac{q^4}{4!}\int_{-\infty}^{\infty} p(x).x^4\,dx + \ldots$$

The analysis is performed on a simulation of finite size with a limited number of realisations and it will be affected by numerical accuracy. Hence it is not unreasonable to assume that the coefficients in this power series do not increase strongly in size for higher order powers; as calculated numerically they are finite. If this is the case then for small enough values of q (necessarily <1) the logarithm of the series may be approximated as

$$\log_e Z(q) \approx -\frac{q^2}{2!}\int_{-\infty}^{\infty} p(x).x^2\,dx.$$

In other words $\mathrm{Re}\,K_I(q) \propto -q^2$. Hence this rather simple argument gives a plausible explanation for how the slope α_I may appear to be 2 for small enough values of q.

III.6.2 Large $C_{1,I}$

The statistics of simulations B and C (both with 1024 realisations) are now evaluated.

The plot for $\mathrm{Re}\{K_{4,I}\}$ is in figure III.12, with α_I=1.8 on the left and α_I=1.5 on the right (simulations B & C respectively). For simulation B (left) the theory (line) is in agreement with the evaluated statistics (points) between q=1.0 & 2.0. For simulation C (right) there is a close agreement only at the single point where q=1.0. The statistics do not follow the theory line for both small and large values of q: the behaviour for large q is characterised by an oscillation in the computed value with a period of 1; for small q the slope is, once again, 2. (The place at which the slope changes slope appears to be at a slightly higher value of q than it did for the corresponding plot of simulation A in figure III.6.)

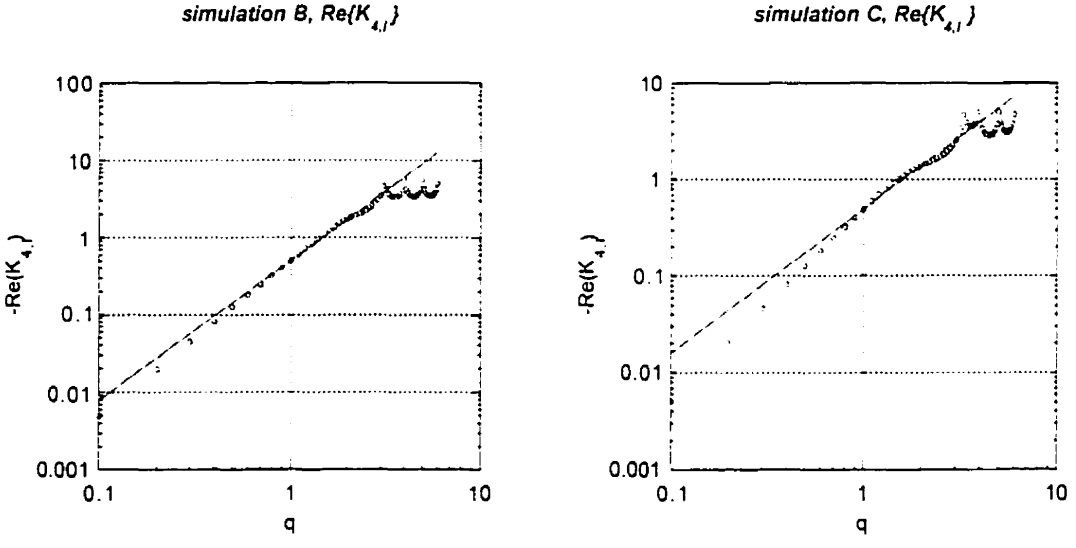

Figure III.12: Plot of $\mathrm{Re}\{K_{4,I}\}$ for simulation B (left) and for simulation C (right) from the bare data in each case. Theory lines, statistics points.

The behaviour for small q has already been described in the previous section. The oscillating effect seen at large values of q can be explained by considering the effect of information loss in the data, or more specifically, by considering the behaviour of the characteristic function of the resulting modified probability density (that is modified due to the loss of information).

In fact a Gaussian distribution will be considered below for mathematical simplicity ie., α_l=2. The variance σ=1.2 is chosen because, for ADPs with λ=4 and using

$$C_{1,l} = -\frac{\sigma^2}{2\log_e \lambda}\left(\frac{\alpha_l - 1}{\cos\frac{\pi\alpha_l}{2}}\right),$$

this gives the effective $C_{1,l}$= $K_1(1)$=0.5194.

The probability density function of a Gaussian r.v., x, may be seen plotted in figure III.13 and is defined by the equation

$$p(x) = \frac{1}{\sigma\sqrt{2\pi}} e^{-x^2/2\sigma^2}.$$

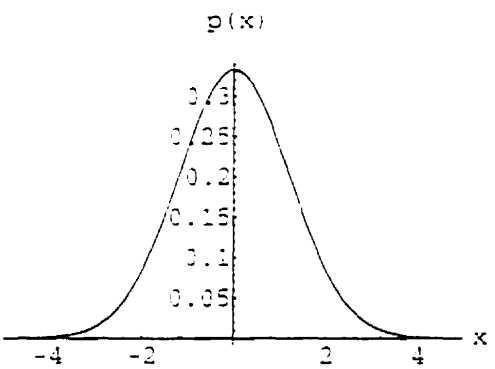

Figure III.13: Plot of p(x) versus x; the p.d.f. of a Gaussian r.v. with variance σ=1.2.

The Fourier transform (F.T.) of p(x) ie., the characteristic function, is $Z(q) = e^{-\sigma^2 q^2/2}$.

The modified p.d.f. can be constructed by taking the sum $p(x) + p'(x)$ ie., where $p'(x)$ is a perturbation to the original p.d.f. Both of these functions can be seen plotted in figure III.14. Note that $p'(x)$ is made up from 2 shifted (by $\pm 2\pi$) and 2 reflected (about the y-axis) 'tail' portions of the original p.d.f. such that the resulting modified p.d.f. is truncated at $\pm\pi$.

The F.T. of $p'(x)$, $Z'(q)$, has been evaluated mathematically using the software package *mathematica* and can be seen plotted in figure III.15 on the left. Note the periodicity of 2, and that after an initial increase in amplitude for low values of q the

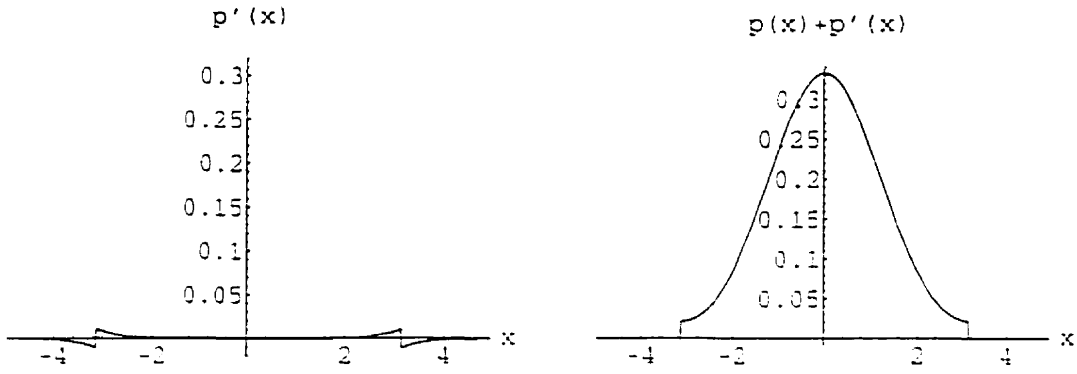

Figure III.14: Plot of $p'(x)$, left, and of the resulting modified p.d.f., $p(x)+p'(x)$, right. (Note that in the plot on the left the y-axis is slightly offset to accommodate the negative excursions.)

function decays slowly as q increases further still. The function has a value of zero for all integer values of q. (Also, since the width of the Gaussian p.d.f. is a function of σ it follows that the amplitude of $Z'(q)$ will increase with increasing σ.)

The resulting characteristic function is simply $Z(q)+Z'(q)$. In practice the logarithm of the absolute value of this quantity is evaluated (to give the second characteristic function) which can be seen in figure III.15 on the right. Note that taking the absolute value doubles the periodicity seen for large q. The perturbation $Z'(q)$ has no effect (on $Z(q)$) at smaller values of q ie., $Z'(q) << Z(q)$ for small q.

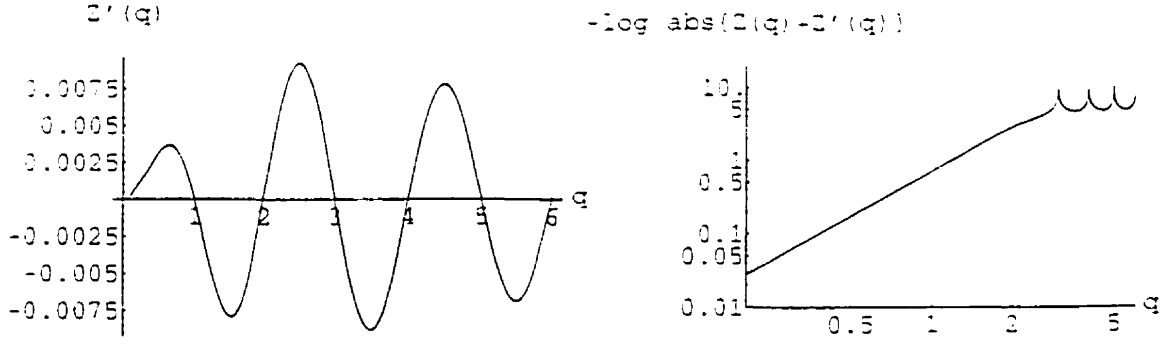

Figure III.15: Plot of the F.T. of $p'(x)$, $Z'(q)$, left, and the second characteristic function of the resulting modified p.d.f., right.

Note that since the amplitude of $Z'(q)$ increases with increasing σ (or $C_{1,I}$) the point at which the perturbation, from the loss of information in the data, will start to be felt (ie., the value of q at which this happens) will be a decreasing function of σ (or $C_{1,I}$).

The final plot which is obtained for the modified second characteristic function can be compared with the plot obtained in figure III.12 (left) for $\mathrm{Re}\{K_{1,I}\}$ for simulation B. (Recall that the parameters in each case are $C_{1,I}=K_I(1)=0.5194$, $\alpha_I=2$ for the theory above and $C_{1,I}=0.4206$, $K_I(1)=0.5$, $\alpha_I=1.8$ for simulation B ie., they differ slightly). The two plots are visibly quite similar.

Hence, with this explanation and the one in § III.6.1, the cause of the limitations in this analysis technique have been demonstrated both for high and low regions of q. However, the point of transition between the affected and unaffected regions (as a function of q) remains a non-trivial function of the underlying statistical parameters, the resolution and the sampling dimension of the data. It is beyond the scope of this thesis to investigate what this relationship may be. What is clear is that as $C_{1,I}$ increases the analysis becomes increasingly affected such that for large enough values of $C_{1,I}$ it will no longer be possible to recover the values of $C_{1,I}$ & α_I. Though, of course, the value of $K_I(1)$ may still be determined by this method.

In conclusion it has been seen that for small values of $C_{1,I}$ the analysis, for the bare data, of z_4 gives good statistical results. For larger values of $C_{1,I}$ the region (in q-space) over which the analysis continues to work is reduced significantly. The exact dependence of the size of this region on the underlying statistical parameters is not known. But provided $C_{1,I}$ is small enough an accurate estimate of $C_{1,I}$ & α_I may be recovered from the plot of $\mathrm{Re}\{K_{1,I}\}$. Notably this analysis method allows the value of α_I to be recovered for larger values of $C_{1,I}$ than does the trace moments method. In addition the consistency of the results may be checked by comparing the values of $K_I(1)$ recovered by this and the trace moments methods.

III.7 Concluding Remarks

The final conclusion from the testing in §§ III.5-6 is that when $C_{1,I}$ is large it becomes very difficult to recover the statistical parameters of the data. This is because of information loss in the complex generator part of the field. The result is that the usual analysis technique (of trace moments) becomes restricted, especially since the process of degrading the data no longer conserves the statistics of the process. The ADP method, developed in this chapter, is capable of extending the useful analysis range to higher values of $C_{1,I}$, but this still has its limitations. Tests have not been performed for empirical estimates of the useful parameter ranges over which the analyses will continue to function.

To sum up, the parameters which may be recovered by the analysis of complex data are:

i) For K_R at the highest resolution (bare data) $K_I(1)$, $C_{1,R}$ and α_R can be recovered (even for large values of $C_{1,I}$), and
ii) the analysis of z_4 at the highest resolution (bare data) for the statistics of $\mathrm{Re}\{K_{4,I}\}$ recovers $K_I(1)$ and will recover $C_{1,I}$ & α_I if $C_{1,I}$ is small enough.

However the full physical significance of the quantity $K_I(1)$ is not known. Neither is it certain whether there may be a physical interpretation of $C_{1,I}$ as the codimension of the imaginary part of the process.

The analyses that have been performed were done so on computer simulations with well-defined statistical properties conforming with the theory. They have demonstrated the limitations that occur when analysing this kind of 'perfect' data. The analysis of recorded data is another matter altogether because there are many additional processes going on which can disturb the analysis significantly. Of the well-established kind there is non-conservation which may be expected to occur in general. Non-conservative complex cascades have not been considered in this thesis but it may be that introducing non-conservation into the theory is a relatively simple exercise. Likewise empirical tests could be performed to determine if fractional complex differentiation preserves the statistical characteristics of a non-conservative complex cascade process.

Of a more serious nature is the question of the arbitrary offset in the recorded data which can totally spoil the evaluated statistics. For example a temperature measurement may be made in degrees Celsius or Kelvin, the difference between the two being a shift in scale of 273.15 units. At this time it is not obvious how to remove such a shift when analysing the data (except by taking differences eg., in structure functions). A similar problem may exist with an arbitrary power to which each field (value) has been raised, and even the question of normalisation is not trivial in the complex plane (because no point is special like the point at unit distance from the origin on the real positive half-line). Some of these problems are removed by using the ADP method (ie., normalisation), but not the serious problems.

Finally it is quite possible that the arbitrary choice of representing a two variable field as the real and imaginary parts of a complex number, in a complex cascade, may turn out to be quite inappropriate for real-life situations. This choice is quite restrictive and probably an over-simplification (and yet see what difficulties it still presents) of reality. The more general Lie cascade representation brings with it even more troublesome 'losses of information' which have so far proved impossible to mitigate. Whether the complex cascade is appropriate or not may finally be determined when the analysis difficulties mentioned above have been removed or circumvented. Apart from this question it should be kept in mind that the very general Lie cascade model is slowly being worked on and that eventually it may be developed to the point where it can be used conclusively.

So finally it may be understood that, due to these difficulties, the attempts which were made at analysing recorded data have so far proved of little use. However it may be expected that in the future a more thorough exposition of the properties of Lie cascades will be made, and with it the complex cascade being a special case thereof. It is the author's hope that this thesis will go some way towards making it easier for anyone choosing to work on this problem to see what has been done, what could not be done, and what still needs to be done.

IV Conclusion

The objective of this thesis has been to elucidate the details of cascade models producing universal multifractal fields and subsequently to investigate the simulation and analysis of these fields in the scalar and complex cases. This has been achieved as follows:

In chapter I the historical development of cascade models has been presented using the specific example of turbulence, showing the progress that has been made in producing models capable of giving ever more realistic characterisations of naturally occurring scaling and multiscaling fields (§§ I.4-5). This progression is punctuated by the development of multifractal models, the discovery of an universal multifractal form, and finally the general multivariate Lie cascade model. The universal m.f. model has been chosen for the work in chapters II-III as being the most realistic and the most amenable to the treatment of multivariate fields.

In chapter II the basic properties of Lévy r.v.s, the building blocks of the universal m.f. cascade, have been described (§ II.2.3) along with some simulations of these r.v.s. The theory for the discrete cascade universal m.f. (DCUM) model has been developed (§ II.2.4) and simulations and analysis of DCUM fields have been presented (§ II.4). There is some discussion on the limitations of the software and analysis (§ II.4.3), though no serious problems are encountered which would make their use untenable later on.

In chapter III the chosen subject is the complex cascade model, being the most simple generalisation of the scalar cascade model. The theory developed in this chapter (§ III.2) closely follows Schertzer & Lovejoy (1995) (though it differs in some minor details for various reasons.) Examples of simulations of complex DCUM fields have been presented (§ III.5-6). Two analysis techniques which can be applied to complex data have been described (§ III.4), one of these being the new "adjacent data points" (ADP) method (§ III.4.3). These analysis techniques have been applied to the complex simulations and it was found that the ADP method is an improvement over the traditional analysis method. A theoretical explanation for the limitations in the analysis of the complex data has also been

demonstrated (§ III.6). Finally the difficulties of analysing recorded data, rather than the 'perfect' data of a simulation, have been discussed (§ III.7).

The unique contributions to knowledge which have arisen from this work are: A considerable understanding of the basic properties of complex cascades has been reached; some of the fundamental limitations of the analysis of complex data have been understood; a new analysis technique, the ADP method, has been developed which is an improvement over the traditional analysis technique (for the analysis of complex data).

A Appendix

The main software routines which have been used to generate the various random variables and fields appearing in this thesis can be found in this appendix for reference.

A.1 Lévy r.v. simulation routines

The function `lvns(long *inum,double alpha,double c)` in § A.1.1 below can be used to generate totally skewed left (β=-1) Lévy r.v.s, x, with parameters α=alpha, $|C_1/(\alpha-1)|$=c and shift parameter μ=0 ie.,

$$\left\langle e^{qx} \right\rangle = e^{C_1 q^\alpha/(\alpha-1)}.$$

The r.v. is stored at memory location `inum`: this function is called by the software in file `dsc_03.h` (§ A.2) which generates a scalar DCUM field. The function `clvns(long *inum,double alpha,double c)` is identical, except that the r.v. produced has a different scale parameter such that

$$\left\langle e^{qx} \right\rangle = e^{q^\alpha/\cos(\pi\alpha/2)},$$

and it is called by the software in file `cpx_03.h` (§ A.3.1) which generates a complex DCUM field.

Note that the function `rst_04.c` and its associated functions of § A.1.2 are modified versions of the functions appearing in Samorodnitsky and Taqqu (1994) on pp. 46-49 rewritten in C.

A.1.1 file "lvnst.h"

```
/*lvnst.h */

#define BETA -1.0


#include <math.h>
#include <stdlib.h>
```

```
#include "include/RAN3.C"                    (numerical recipes routine)
#include "include/rst_04.c"


dcuble lvns(long *inum,double alpha,dcuble c)
{
      double offset,a,b;


      if(alpha!=1.0)
      {
            offset=BETA*tan(M_PI_2*alpha);
            c=c*cos(M_PI_2*alpha);
            if(c<0)
                  c=-c;
            c=pow(c,1.0/alpha);
      }
      else
      {
            c=c*M_PI_2;
            offset=0.0;
      }

      a=(double)ran3(inum);
      if(a==0.0||a==1.0)
            a=(double)ran3(inum); /* assume it does not repeat */
      b=(double)ran3(inum);
      if(b==0.0||b==1.0)
            b=(double)ran3(inum); /* ditto */
      b=-log(b);

      return c*(rstable(alpha,BETA,a,b)+offset);
}


/* for use as exp(i*lvns) (ie., imaginary) */
double clvns(long *inum,double alpha,double c)
{
      double offset,a,b;
```

```
        if(alpha!=1.0)
        {
                offset=BETA*tan(M_PI_2*alpha);
                if(c<0)
                        c=-c;
                c=pow(c,1.0/alpha);
        }
        else
                offset=0.0;

        a=ran3(inum);
        b=-log(ran3(inum));

        return c*(rstable(alpha,BETA,a,b)+offset);
}

#undef BETA
```

A.1.2 file "rst_04.c" and associated functions

```
/* rst_04.c adapted from S&T pp. 46-48 */

#include <math.h>
#include <stdlib.h>

#include "include/truth.h"

double rstable(double alpha,double bprime,double u,double w)
{
        double phiby2,a,eps,b;
        double bb,tau,a2,a2p,b2,b2p,alogz,z,d,st,rstabl;
        double tan2d(double xarg);
        double d2d(double z);

        eps=1.0-alpha;
        phiby2=M_PI_2*(u-0.5);
        a=phiby2*tan2d(phiby2);
        bb=tan2d(eps*phiby2);
        b=eps*phiby2*bb;
        if(eps>-0.99)
```

```
            tau=bprime/(tan2d(eps*M_PI_2)*M_PI_2);
      if(eps<=-0.99)
            tau=bprime*M_PI_2*eps*(1.0-eps)*tan2d((1.0-eps)*M_PI_2);

      a2=a*a;
      a2p=1.0+a2;
      a2=1.0-a2;
      b2=b*b;
      b2p=1.0+b2;
      b2=1.0-b2;

      z=a2p*(b2+2.0*phiby2*bb*tau)/(w*a2*b2p);

      alogz=log(z);
      d=d2d(eps*alogz/(1.0-eps))*(alogz/(1.0-eps));

      rstabl=(1.0+eps*d)*2.0*((a-b)*(1.0+a*b)-
            phiby2*tau*bb*(b*a2-2.0*a))/(a2*b2p)+tau*d;

      return rstabl;
}


#define P1 0.840066852536483239e3
#define P2 0.200011141589964569e2
#define Q1 0.168013370507296648e4
#define Q2 0.180013370407390023e3
#define Q3 1.0

double d2d(double z)
{
      double pv,zz,d2;

      if(fabs(z)>0.1)
            d2=(exp(z)-1.0)/z;
      else
      {
            zz=z*z;
            pv=P1+zz*P2;
            d2=2.0*pv/(Q1+zz*(Q2+zz*Q3)-z*pv);
```

```
        }

        return d2;
}

#undef P1
#undef P2
#undef Q1
#undef Q2
#undef Q3


#define P0 0.129221035031569917e3
#define P1 -0.8876623770211723e1
#define P2 0.528644455522248e-1
#define Q0 0.164529331810168605e3
#define Q1 -0.4513205610059896le2

double mytand(double xarg) /* adapted from S&T p. 46 */
{
        double mytan;
        int neg,inv;
        double x,xx;

        neg=FALSE;
        inv=FALSE;

        x=xarg;
        if(x<0.0)
                neg=TRUE;
        x=fabs(x);

        if(x>M_PI_4) {
                x=fmod(x,M_PI);
                if(x>M_PI_2) {
                        neg^=TRUE;
                        x=M_PI-x;
                }
                if(x>M_PI_4) {
                        inv=TRUE;
```

```
                x=M_PI_2-x;
            }
        }
        x/=M_PI_4;
        xx=x*x;
        mytan=x*(P0+xx*(P1+xx*P2))/(Q0+xx*(Q1+xx));
        if(neg)
            mytan=-mytan;
        if(inv)
            mytan=1.0/mytan;

        return mytan;
}


double tan2d(double xarg) /* adapted from S&T pp. 48-49 */
{
        double x,xx,tan2;

        x=fabs(xarg);
        if(x>M_PI_4)
            tan2=mytand(xarg)/xarg;
        else
        {
            x/=M_PI_4;
            xx=x*x;
            tan2=(P0+xx*(P1+xx*P2))/(M_PI_4*(Q0+xx*(Q1+xx)));
        }

        return tan2;
}

#undef P0
#undef P1
#undef P2
#undef Q0
#undef Q1
```

A.1.3 file "truth.h"

```
#ifndef __truth_h__
#define __truth_h__

#define TRUE 1
#define FALSE 0

#endif /* __truth_h__ */
```

A.2 Scalar DCUM simulation routine

The function dsc(double *deg,long *inum,long size,double alpha,double c) below produces a scalar DCUM field, ε_λ, of resolution λ where $\log_2 \lambda$=size at memory location deg (the memory at inum is used internally). It has the parameters α=alpha and $C_1/(\alpha-1)$=c such that

$$\left\langle \varepsilon_\lambda^q \right\rangle = \exp\left\{ \frac{C_1}{\alpha - 1}(q^\alpha - q)\log_e \lambda \right\}.$$

```
/* dsc_03.h discrete scalar cascade simulation */

#define E0 1.0 /* epsilon naught */

#include <stdio.h>
#include <unistd.h>
#include <fcntl.h>
#include <sys/stat.h>
#include <sys/types.h>
#include <stdlib.h>
#include <math.h>

#include "include/lvnst.h"


void dsc(double *deg,long *inum,long size,double alpha,double c)
{
      long count0,count1,last;
```

```
double data_array[23];
long ratio=sizeof(*data_array);
double *dp;
long total;
double u,un;
double levy;
double factor,offset;

u=M_LN2;

if(c<=0.0)
{
      printf("invalid c\n");
      exit(1);
}
un=pow(u,(1.0/(double)alpha-1.0));


total=(1<<size);

if(alpha!=1.0)
      offset=c;
else
      offset=0.0;
if(alpha!=1.0)
      offset=c;
else
      offset=0.0;

data_array[0]=E0;


for(count0=1;count0<=size;count0++)
{
      levy=u*((lvns(inum,alpha,c)*un)-offset);
      data_array[count0]=data_array[count0-1]*exp(levy);
}

dp=deg;
*dp++=data_array[size];
```

```
        last=0;
        for(count1=1;count1<total;count1++)
        {
                for(count0=1;count0<=size;count0++)
                {
                        if((count1^last)&(1L<<(size-count0)))
                        {
                                levy=u*((lvns(inum,alpha,c)*un)-offset);
                                data_array[count0]=data_array[count0-
                                        1]*exp(levy);
                        }
                }
                *dp++=data_array[size];
                last=count1;
        }


        return;
}

#undef E0
```

A.3 Complex DCUM simulation routine

The function `cpx(double *deg[2],long *inum,long size,float alpha[2], float c[2])` in § A.3.1 produces a complex DCUM field, ε_λ, of resolution λ where $\log_2 \lambda$=`size` with the real part at memory location `deg[0]` and the imaginary part at `deg[1]` (the memory at `inum` is used internally). It has the parameters α_R=`alpha[0]` & α_I=`alpha[1]` and $\left|C_{1.R}/(\alpha_R-1)\right|$=`c[0]` & $\left|\left\{C_{1.I}/(\alpha_I-1)\right\}\cos(\pi\alpha_I/2)\right|$= `c[0]` such that for $q>0$

$$\left\langle \varepsilon_\lambda^q \right\rangle = \exp\left[\left\{\frac{C_{1.R}}{\alpha_R-1}(q^{\alpha_R}-q)+\frac{C_{1.I}}{\alpha_I-1}(q^{\alpha_I}-q)\cos\frac{\pi\alpha_I}{2}+i\frac{C_{1.I}}{\alpha_I-1}(q^{\alpha_I}-q)\sin\frac{\pi\alpha_I}{2}\right\}\log_e\lambda\right]$$

A.3.1 file "cpx_03.h"

```
/* cpx_03.h direct complex cascade simulation */

#define V0 M_SQRT1_2
#define V1 M_SQRT1_2

#include <stdio.h>
#include <unistd.h>
#include <fcntl.h>
#include <sys/stat.h>
#include <sys/types.h>
#include <stdlib.h>
#include <math.h>

#include "include/mv_01.c"
#include "include/lvnst.h"


void cpx(double *deg[2],long *inum,long size,float alpha[2],float c[2])
{
      long count0,count1,last;
      long ratio=8;
      double data_array[23][2];
      double *dp0,*dp1;
      long total;
      double M[2][2];
      double u,un[2];
      double levy[2];
      double factor[2],offset[2];

      u=M_LN2;

      for(count0=0;count0<2;count0++)
      {
            if(c[count0]<=0.0)
            {
                  printf("invalid c\n");
                  exit(1);
            }
            un[count0]=pow(u,(1.0/(double)alpha[count0])-1.0);
```

```
}


total=(1<<size);

if(alpha[0]!=1.0)
      offset[0]=-c[0]+c[1];
else
      offset[0]=0.0;
if(alpha[1]!=1.0)
      offset[1]=c[1]*tan(M_PI_2*alpha[1]);
else
      offset[1]=0.0;

data_array[0][0]=V0;
data_array[0][1]=V1;


for(count0=1;count0<=size;count0++)
{
      levy[0]=(lvns(inum,alpha[0],c[0])*un[0])+offset[0];
      levy[1]=(clvns(inum,alpha[1],c[1])*un[1])+offset[1];

      mrot(u*levy[1],M);
      msm(exp(u*levy[0]),M);

      mv(M,data_array[count0-1],data_array[count0]);
}

dp0=&deg[0][0];
dp1=&deg[1][0];

*dp0++=data_array[size][0];
*dp1++=data_array[size][1];


last=0;
for(count1=1;count1<total;count1++)
{
      for(count0=1;count0<=size;count0++)
```

```
            {
                  if((count1^last)&(1L<<(size-count0)))
                  {

      levy[0]=(lvns(inum,alpha[0],c[0])*un[0])+offset[0];

      levy[1]=(clvns(inum,alpha[1],c[1])*un[1])+offset[1];

                        mrot(u*levy[1],M);
                        msm(exp(u*levy[0]),M);

                        mv(M,data_array[count0-1],data_array[count0]);
                  }
            }
                *dp0++=data_array[size][0];
                *dp1++=data_array[size][1];

            last=count1;
      }

      return;
}

#undef V0
#undef V1
```

A.3.2 file "mv_01.c"

```
/* mv_01.c contains matrix functions */

#include <math.h>


/* qQ (scalar and matrix product a=q*a) */
void msm(double q, double a[2][2])
{
      a[0][0]*=q;
      a[1][1]*=q;
      a[0][1]*=q;
      a[1][0]*=q;
```

```
}

/* matrix times column vector w=a*v */
void mv(double a[2][2], double v[2], double w[2])
{
      w[0]=(a[0][0]*v[0])+(a[0][1]*v[1]);
      w[1]=(a[1][0]*v[0])+(a[1][1]*v[1]);
}

/* rotation matrix a(theta) */
void mrot(double theta,double a[2][2])
{
      a[1][1]=a[0][0]=cos(theta);
      a[1][0]=sin(theta);
      a[0][1]=-a[1][0];

      return;
}
```

Bibliography

Anselmet, F., Gagne, Y., Hopfinger, E.J., Antonia, R.A., 1984. *High-Order Velocity Structure Functions in Turbulent Shear Flows,* J. Fluid Mech. **140**, 63-89

Arneodo, A., Baudet, C., Belin, F., Benzi, R., Castaing, B., et al., 1996. *Structure Functions in Turbulence, in Various Flow Configurations, at Reynolds Number Between 30 and 5000, Using Extended Self-Similarity,* Europhys. Lett. **34**, 411-416

Batchelor, G.K., Townsend, A.A., 1949. *The Nature of Turbulent Motion at Large Wave-Numbers,* Proc. R. Soc. Lond. A, **199** 238-255

Benzi, R., Ciliberto, S., Tripiccione, R., Baudet, C., Massaioli, F., Succi, S., 1993. *Extended Self-Similarity in Turbulent Flows,* Amer. Phys. Soc. **48**, R29-R32

Benzi, R., Paladin, G., Parisi, G., Vulpiani, A., 1984. *On the Multifractal Nature of Fully Developed Turbulence and Chaotic Sustems,* J. Phys. **A17**, 3521-3531

Bhattacharjee, J.K., 1998. *The Problem of Turbulence,* Indian J. Phys **72B**, 383-405

Campbell, J., 1960. *The Masks of God: Primitive Mythology,* Secker & Warburg, London

Cantor, G., 1883. *Grundlagen Einer Allgemeinen Mannichfältigkeitslehre,* Math. Ann. **21**, 545-591

Chambers, J.M., Mallows, C., Stuck, B.W., 1976. *A Method for Simulating Stable Random Variables,* J. Amer. Stat. Assoc. **71**, 340-344

Chigirinskaya, Y., Scherzter, D., 1996. *Cascade of Scaling Gyroscopes: Lie Structure, Universal Multifractals and Self-Organized Criticality in Turbulence,* in Stochastic Models in Geophysics, A. Molchanov, W.A. Woyczynski eds., Springer-Verlag, New York

Desaulniers-Soucy, N., Iuoras, I., 1999. *Traffic Modeling with Universal Multifractals,* submitted to Globe Comm. Conf. 1999

Einstein, A., 1905. *Zur Elektrodynamik Bewegter Körper,* Ann. Phys. **17**, 891-921

Feder, J., 1988. *Fractals,* Plenum Press, New York

Feller, W., 1966. *An Introduction to Probability Theory and its Applications,* **II**, John Wiley & Sons, New York

Frisch, U., 1995. *Turbulence: The Legacy of A.N. Kolmogorov,* Cambridge Univ. Press, Cambridge

Frisch, U., Sulem, P.L., Nelkin, M., 1978. *A Simple Dynamical Model of Intermittent Fully Developed Turbulence,* J. Fluid Mech. **87**, 719-736

Gargett, A.E., 1989. *Ocean Turbulence,* Ann. Rev. Fluid Mech. **21**, 419-451

Gledzer, E.B., 1973. *System of Hydrodynamic Type Admitting Two Quadratic Integrals of Motion,* Dokl. Akad. Nauk. SSSR, 1046-1048 (reprinted in English in Sov. Phys. Dokl. (1973) **18**, 216-217)

Gödel, K., 1931. *Über Formal Unentscheidbare Sätze der Principia Mathematica und Verwandter Systeme, I,* Monatshefte für Mathematik und Physik **31**, 173-198

Grant, H.L., Stewart, R.W., Moilliet, A., 1962. *Turbulent Spectra From a Tidal Channel,* J. Fluid Mech. **12**, 241-268

Hentschel, H.G.E., Procaccia, I., 1983. *The Infinite Number of Generalized Dimensions of Fractals and Strange Attractors,* Physica **D8**, 434-444

Hilbert, D., 1900. *Mathematische Probleme,* Göttinger Nachrichten 253-297 (reprinted in English in Mathematical Developments Arising from Hilbert Problems, (1976) F. Brouder ed., American Mathematical Society, Providence)

Janicki, A., Weron, A., 1994. *Simulation and Chaotic Behaviour of α-Stable Stochastic Processes,* Marcel Dekker, New York

Johnson, P., 1996. *Modern Times: A History of the World From the 1920s to the 1990s,* p. 5, Phoenix, London

Kelvin , Lord (Thomson, Sir W.), 1887. *On the Propagation of Laminar Motion Through a Turbulently Moving Inviscid Liquid,* Phil. Mag. S. 5, **24**, 342-353

Kendall, D.G., 1990. *Kolmogorov: The Man and his Work,* Bull. Lond. Math. Soc. **22**, 31-47

Kolmogorov, A.N., 1941a. *The Local Structure of Turbulence in Incompressible Viscous Fluid for Very Large Reynolds Numbers,* Dokl. Akad. Nauk. SSSR **30**, 9-13 (reprinted in English in Proc. R. Soc. Lond. A (1991) **434**, 9-13)

Kolmogorov, A.N., 1941b. *Dissipation of Energy in the Locally Isotropic Turbulence,* Dokl. Akad. Nauk. SSSR **32**, 16-18 (reprinted in English in Proc. R. Soc. Lond. A (1991) **434**, 15-17)

Kolmogorov, A.N., 1962. *A Refinement of Previous Hypotheses Concerning the Local Structure of Turbulence in a Viscous Incompressible Fluid at High Reynolds Number,*

J. Fluid Mech. **13**, 82-85 (translation of a lecture given at the Coll. Int. du CNRS de Mécanique de la Turbulence, 1961, Marseilles)

Lavallée, D., 1991. *Multifractal Analysis and Simulation Techniques and Turbulent Fields*, PhD thesis, McGill University, Montréal

Leveque, E., She, Z-S., 1997. *Cascade Structure and Scaling Exponents in a Dynamical Model of Turbulence: Measurements and Comparison*, Phys. Rev. E **55**, 2789-2799

Lilly, D.K., 1983. *Meso-scale Variability of the Atmosphere*, in Meso-scale Meteorology —Theories, Observations and Models, 13-24, D.K. Lilly and T. Gal-Chen eds., D. Reidel, New York

Lorenz, E.N., 1963. *Deterministic Nonperiodic Flow*, J. Atm. Sci. **20**, 130-141

Lovejoy, S., Schertzer, D., 1995. *How Bright is the Coast of Brittany?* in Image Understanding Research vol. 1, 102-151, G. Wilkinson, I. Kanellopoulos, J. Mégier eds., Institute for Remote Sensing Applications, Proc. of Joint JRC/EARSeL Expert Meeting, Ispra, Italy, April 1994, ECSC-EC-EAEC, Brussels

Lugt, H.J., 1983. *Vortex Flow in Nature and Technology*, John Wiley & Sons, New York

Mandelbrot, B.B., 1967. *How Long is the Coast of Britain?* Statistical Self-Similarity and Fractional Dimension, Science **156**, 636-638

Meakin, P., 1998. *Fractals, Scaling and Growth Far From Equilibrium*, Cambridge University Press, Cambridge

Meneveau, C., Sreenivasan, K.R., 1987. *Simple Multifractal Cascade Model for Fully Developed Turbulence*, Phys. Rev. Lett. **59**, 1424-1427

Navier, C.L.M.H., 1823. *Mémoire sur les Lois du Mouvement des Fluids*, Mém. Acad. Roy. Sci. **6**, 389-440

Novikov, E.A., Stewart, R.W., 1964. *The Intermittency of Turbulence and the Spectrum of Energy Dissipation*, Izv. Akad. Nauk. SSSR Ser. Geofiz. **3**, 408-413

Oboukhov, A.M., 1941. *On the Distribution of Energy in the Spectrum of Turbulent Flow*, Dokl. Akad. Nauk. SSSR **32**, 22-24

Oboukhov, A.M., 1962. *Some Specific Features of Atmospheric Turbulence*, J. Fluid Mech. **13**, 77-81

O'Connor, J.J., Robertson, E.F., 1999. *The MacTutor History of Mathematics archive*, http://www-groups.dcs.st-and.ac.uk/~history/

Ott, E., Yunson, D., Sreenivasan, K.R., Juneja, A., Suri, A.K., 1992. *Sign-Singular Measures: Fast Magnetic Dynamos, and High-Reynolds-Number Fluid Turbulence,* Phys. Rev. Lett. **69**, 2654-2657

Parisi, G., Frisch, U., 1985. *On the Singularity Structure of Fully Developed Turbulence,* in Turbulence and Predictability in Geophysical Fluid Dynamics and Climate Dynamics, 84-88, M. Ghil, R. Benzi & G. Parisi eds., North-Holland, New York

Planck, M., 1900. *Zur Theorie des Gesetzes der Energieverteilung im Normalspektrum,* Verhandlungen der Deutschen Physikalischen Gesellschaft **2**, 237-245 (also as *Über das Gesetz der Energieverteilung im Normalspektrum,* Ann. Phys. **4**, 553-563, 1901)

Poincaré, H., 1892. *Les Méthodes Nouvelles de la Méchanique Celeste,* Gauthier-Villars, Paris

Press, W.H., Teukolsky, S.A., Vetterling, W.T., Flannery, B.P., 1988. *Numerical Recipes in C: The Art of Scientific Computing,* 2nd ed., Cambridge Univ. Press, Cambridge

Reynolds, O., 1883. *An Experimental Investigation of the Circumstances Which Determine Whether the Motion of Water Shall be Direct or Sinuous, and of the Law of Resistance in Parallel Channels,* Philos. Trans. Roy. Soc. Lond. **174**, 935-982

Richardson, L.F., 1922. *Weather Prediction By Numerical Process,* Cambridge Univ. Press, Cambridge

Riedi, R.H, Scheuring, I., 1997. *Conditional and Relative Multifractal Spectra,* Fractals **5**, 153-168

Samorodnitsky, G., Taqqu, M.S., 1994. *Stable Non-Gaussian Random Processes: Stochastic Models with Infinite Variance,* Chapman & Hall, New York

Schertzer, D., Lovejoy, S., 1984. *On the Dimension of Atmospheric Motions,* in Turbulence and Chaotic Phenomena in Fluids, 505-512, T. Tatsumi ed., North-Holland, New York

Schertzer, D., Lovejoy, S., 1985. *The Dimension and Intermittency of Atmospheric Dynamics,* Turbulent Shear Flow **4**, 7-33, B. Launder ed., Springer, New York

Schertzer, D., Lovejoy, S., 1987. *Physical Modeling and Analysis of Rain and Clouds by Anisotropic Scaling Multiplicative Processes,* J. Geophys. Res. **92**, 9693-9714

Schertzer, D., Lovejoy, S., 1995. *From Scalar Cascades to Lie Cascades: Joint Multifractal Analysis of Rain and Cloud Processes,* in Space/Time Variability and

Interdependence for Various Hydrological Processes, 153-173, R.A. Feddes ed., Cambridge Univ. Press, Cambridge

Schertzer, D., Lovejoy, S., 1996. *A Short Course in Multifractals*, McGill University, Montréal

Schertzer, D., Lovejoy, S., 1999. *Generalized Stable Multivariate Distribution and Anisotropic Dilatations*, in preparation for J. Multivariate Analysis

Schertzer, D., Lovejoy, S., Schmitt, F., 1995. *Structures in Turbulence and Multifractal Universality*, in Small-Scale Structures in Three-Dimensional Hydro and Magnetohydrodynamic Turbulence, A. Meneguzzi, A. Pouquet, P.L. Sulem eds., in Lecture Notes in Physics, **462**, 137-144, Springer-Verlag, Berlin

Schertzer, D., Lovejoy, S., Schmitt, F., Chigirinskaya, Y., Marsan, D., 1997. *Multifractal Cascade Dynamics and Turbulent Intermittency*, Fractals **5** 427-471

Seed, A., 1989. *Statistical Problems in Measuring Convective Rainfall*, PhD thesis, McGill University, Montréal

She, Z-S., Leveque, E., 1994. *Universal Scaling Laws in Fully Developed Turbulence*, Phys. Rev. Lett. **72**, 336-339

Sreenivasan, K.R., 1991. *Fractals and Multifractals in Fluid Turbulence*, Annu. Rev. Fluid Mech. **23**, 539-600

Sreenivasan, K.R., Antonia, R.A., 1997. *The Phenomenology of Small-Scale Turbulence*, Annu. Rev. Fluid Mech. **29**, 435-472

Taylor, G.I., 1935. *Statistical Theory of Turbulence*, Proc. Roy. Soc. Lond. A. **151**, 421-478

Townend,H.C.H. , 1934. *Statistical Measurements of Turbulence in the Flow of Air Through a Pipe*, Proc. Roy. Soc. Lond. A. **145**, 180-211

Truesdell, C., 1968. *Essays in the History of Mechanics*, Springer-Verlag, New York

Vainshtein, S.I., Sreenivasan, K.R., 1994. *Kolmogorov's 4/5th Law and Intermittency in Turbulence*, Phys. Rev. Lett. **73**, 3085-3088

Van Atta, C.W., Park, J., 1970. *Structure Functions of Turbulence in the Atmospheric Boundary Layer Over the Ocean*, J. Fluid Mech. **44**, 145-159

Van Dyke, M., 1982. *An Album of Fluid Motion*, The Parabolic Press, Stanford

Van der Hoven, J., 1957. *Power Spectrum of Horizontal Wind Speed in the Frequency Range From 0.0007 to 900 cycles per hour*, J. Meteor. **14**, 160-164

Von Koch, H., 1906. *Une Méthode Géometrique Élémentaire pour l'Étude de Certaines Questions de la Théorie des Courbes Planes,* Acta Math. **30**, 145-174

Warn, T., 1995. *Turbulence Course Notes,* ch. 1, p. 1, unpublished

Wyngaard, J.C., 1991. *Atmospheric Turbulence,* Annu. Rev. Fluid Mech. **24**, 205-233

Yaglom, A.M., 1966. *The Influence of Fluctuations in Energy Dissipation on the Shape of Turbulence Characteristics in the Inertial Interval,* Dokl. Akad. Nauk. SSSR **166**, 49-52 (reprinted in English in Sov. Phys. Dokl. (1966) **11**, 26-29)

Yamada, M., Ohkitani, K., 1987. *Lyapunov Spectrum of a Chaotic Model of Three-Dimensional Turbulence,* J. Phys. Soc. Japan **56**, 4210-4213

Zolotarev, V.M., 1983. *One-Dimensional Stable Distributions,* Nauka, Moscow (English translation is One-Dimensional Stable Distributions, Translations of Mathematical Monographs (1986) **65**, American Math. Soc, Providence)